Finite volume methods for the computation of statistical solutions of the incompressible Euler equations

C. Parés-Pulido

Finite volume methods for the computation of statistical solutions of the incompressible Euler equations

Carlos Parés-Pulido[*], Seminar for Applied Mathematics, ETH Zurich

September 29, 2021

Abstract

We present an efficient numerical scheme based on Monte Carlo integration to approximate statistical solutions of the incompressible Euler equations. The scheme is based on finite volume methods, which provide a more flexible framework than previously existing spectral methods for the computation of statistical solutions for incompressible flows. This finite volume scheme is rigorously proven to, under experimentally verifiable assumptions, converge in an appropriate topology and with increasing resolution to a statistical solution. The convergence obtained is stronger than that of measure-valued solutions, as it implies convergence of multi-point correlation marginals. We present results of numerical experiments which support the claim that the aforementioned assumptions are very natural, and appear to hold in practice.

Keywords: incompressible fluid dynamics; statistical solutions; partial differential equations.

1 Introduction

The formal limit of the Navier–Stokes equations as the ***Reynolds number*** tends to infinity produces the ***incompressible Euler equations***, classically written as

$$\begin{cases} \partial_t \boldsymbol{u} + \boldsymbol{u} \cdot \nabla \boldsymbol{u} + \nabla p = 0, \\ \operatorname{div}(\boldsymbol{u}) = 0, \\ \boldsymbol{u}|_{t=0} = \overline{\boldsymbol{u}}; \end{cases}$$

where $\boldsymbol{u} \in \mathbb{R}^d$ ($d \in \{2,3\}$) is the fluid velocity, $p \in [0,\infty)$ is the pressure, and $\overline{\boldsymbol{u}}$ is a known initial condition in some function space to be detailed. We will consider these equations defined on a finite time domain $[0,T]$ for $T > 0$, and a spatial domain D which we will always take to have periodic boundary conditions; i.e., $D = \mathbb{T}^d$. These equations are widely used to model turbulent flows, in which the Reynolds number is large.

---

[*] *carlos.pares-pulido@sam.math.ethz.ch*, Rämistrasse 101, Zürich, Switzerland

1.1 Existence and uniqueness of solutions

The problem of existence and uniqueness of classical (i.e. differentiable) solutions of the equations of motion for incompressible fluids is, in a general setting, an open question; cf. Fefferman (2006). For the incompressible Euler equations, in two dimensions and for smooth initial data, it is known that classical solutions exist globally, Ladyzhenskaya (1969), Beale et al. (1984). In three dimensions, however, the only existence results available are local in time, Lichtenstein (1925). Furthermore, the study of non-differentiable initial data (e.g. $\overline{\boldsymbol{u}} \in L^2(D)$) is often of interest. Therefore one often studies the **weak formulation** of the incompressible Euler equations:

Definition 1.1. A vector field $\boldsymbol{u} \in L^\infty([0,T); L^2(D, \mathbb{R}^d))$ is a **weak solution of the incompressible Euler equations** with initial datum $\overline{\boldsymbol{u}} \in L^2(D; \mathbb{R}^d)$, if for all test vector fields $\phi \in C_c^\infty([0,T) \times D; \mathbb{R}^d)$ with $\mathrm{div}(\phi) = 0$, it holds that

$$\int_0^T \int_D [\boldsymbol{u} \cdot \partial_t \phi + (\boldsymbol{u} \otimes \boldsymbol{u}) \colon \nabla \phi] \, dx dt = - \int_D \overline{\boldsymbol{u}} \cdot \phi(0, x) \, dx,$$

and for all test functions $\psi \in C^\infty(D)$,

$$\int_D \boldsymbol{u} \cdot \nabla \psi \, dx = 0.$$

In the equations above, $\otimes$ denotes the tensor product of vectors, and $\colon$ the inner product for matrices.

Existence of weak solutions, globally in time, is a classical result, Leray (1934). Let us recall the concept of vorticity, $\boldsymbol{\eta} \coloneqq \mathrm{curl}(\boldsymbol{u}) \coloneqq \nabla \times \boldsymbol{u}$. In two dimensions, global existence and uniqueness of solutions holds if the initial vorticity $\bar{\boldsymbol{\eta}} \coloneqq \mathrm{curl}(\overline{\boldsymbol{u}})$ verifies $\bar{\boldsymbol{\eta}} \in L^\infty(\mathbb{R}^2)$, Yudovich (1963), or $\bar{\boldsymbol{\eta}} \in L^1(\mathbb{R}^2) \cap L^p(\mathbb{R}^2)$, with $1 < p < \infty$, DiPerna & Majda (1987). Furthermore, global existence of solutions (without uniqueness) is known if the initial vorticity $\bar{\boldsymbol{\eta}} \in H^{-1}(\mathbb{R}^2)$ is of the form $\bar{\boldsymbol{\eta}} = \mu + g$, with $\mu \in \mathcal{M}_+$ a positive Radon measure, and $g \in L^p$, for $p \in [1, \infty]$, Delort (1991), Vecchi & Wu (1993). In the torus, in two and three dimensions, if $\overline{\boldsymbol{u}} \in L^2(\mathbb{T}^d)$, there exist global solutions (in fact, infinitely many) with bounded kinetic energy, Wiedemann (2011).

The results above are representative of the difficulties of uniqueness for weak solutions. In fact, there exists a dense set in $L^2(D; \mathbb{R}^d)$ of so-called **wild initial data**, each of which admits infinitely many weak solutions; De Lellis & Székelyhidi (2009), De Lellis & Székelyhidi (2013). The discontinuous shear layer, which we discuss in detail in Section 5.2, is known to belong to this set, Székelyhidi (2011). Even restricting Definition 1.1 to functions in the class of **admissible weak solutions**, i.e. with non-increasing kinetic energy $\|\boldsymbol{u}\|_{L^2}^2$, uniqueness in a general setting fails.

We remark here the following recent result, due to Lanthaler et al. (2021): a weak solution to the incompressible Euler equations is dubbed **physically realizable** if it is the weak limit in L^2 of a vanishing viscosity sequence of solutions of the incompressible Navier–Stokes equations. In **two spatial dimensions**, physically realizable solutions conserve kinetic energy if and only if they are the **strong limit** in $L^p([0,T]; L^2(D; \mathbb{R}^d))$, $p \geq 1$, of some subsequence of the vanishing viscosity sequence. As wild initial data admit weak solutions which do not conserve energy, this suggests that the aforementioned class might not be physically relevant (in the sense of vanishing viscosity). In three dimensions, however, no analogous result is available, as there exist energy-dissipative solutions which are realizable as a strong vanishing viscosity limit of weak solutions to incompressible Navier–Stokes, Buckmaster & Vicol (2019).

There exist many numerical schemes for the computation of approximate solutions of the incompressible equations of fluid dynamics; a survey can be found e.g. in Langtangen et al. (2002). Of particular interest for this work is the finite volume scheme of Bell et al. (1989), based on a discrete Leray projection. Note that the lack of uniqueness discussed above hinders the application of numerics, regardless of the scheme. If no unique solution exists, numerical schemes may not produce a Cauchy sequence as the resolution increases; this is known to be the case for the Bell–Colella–Glaz scheme. Even for schemes that are provably convergent under sufficient assumptions of regularity, see e.g. Majda & Bertozzi (2001), this convergence is very slow, limiting the practical usefulness of the results.

1.2 Expanded solution spaces for the incompressible Euler equations

The absence of well-posedness results for weak solutions in a general setting, as well as the difficulties for numerical approximations, leave the door open for defining alternative frameworks for solutions. One which has proven popular is that of **measure-valued solutions**, originally presented in DiPerna (1985), DiPerna & Majda (1987), in which the solution is searched for in the space of probability measures parameterized in space and time, i.e. **Young measures**.

Measure-valued solutions of the incompressible Euler equations are known to exist globally, DiPerna & Majda (1987), and there exist efficient algorithms to approximate them (in weak* topology), e.g. via Monte Carlo integration, e.g. Lanthaler & Mishra (2015), Leonardi (2018b), or by Césaro-type averaging of approximations at different resolutions, e.g. Feireisl et al. (2020).

Furthermore, the following **weak-strong uniqueness** property is known for measure-valued solutions, Brenier et al. (2011): for $d \in \{2, 3\}$, if the initial datum $\boldsymbol{u}_0$ is such that a classical solution $\boldsymbol{u}$ exists for all time, then there exists a unique measure-valued solution with $\nu_{t,x} = \delta_{\boldsymbol{u}(t,x)}$. That is, the measure-valued solution takes, at point (t, x) the value of $u(t, x)$ with probability one; this is termed an **atomic measure**.

Measure-valued solutions have, however, poor properties of uniqueness. Even in the simpler case of one-dimensional conservation laws (cf. Example 9.1 in Fjordholm et al. (2016)), it is easy to construct different measure-valued solutions for the same stochastic initial datum. Young measures are pointwise-parameterized probability measures, which can be thought of as marginals of the joint probability measure of the values of the function globally. It is clear that, without additional information about correlations, marginals alone cannot uniquely describe a joint measure.

As a remedy to this lack of uniqueness, the framework of **statistical solutions** has been proposed. Within it, a solution is sought in the space of time-parameterized probability distributions in L^p. There is ample literature on the topic, e.g. Foias (1973), Vishik et al. (1979), Foias et al. (2013). In this work, we will follow the ideas and notation of Fjordholm, Lanthaler & Mishra (2017), in which the authors proved that time-parameterized probability distributions in L^p can be uniquely identified with a **correlation measure**, an infinite hierarchy of Young measures corresponding to the marginal distributions for finite tuples of points. We will define this rigorously in the sequel.

There exist in the literature efficient algorithms for the computation of statistical solutions for hyperbolic conservation laws, both scalar and systems thereof, e.g. Fjordholm et al. (2016, 2020), Lye (2020); as well as for the incompressible Euler equations with spectral hyper-viscosity schemes, Lanthaler et al. (2021). However, to our knowledge, no such method is available for the incompressible Euler equations outside of spectral schemes; this poses strict limitations on the set of spatial domains numerical schemes can be applied to. Hence, the goals of this paper are (a) present the fundamental concepts about sta-

tistical solutions of the incompressible Euler equations; (b) derive a numerical scheme for the practical approximation of the same, based on finite volumes; and (c) rigorously prove that the approximations produced by this scheme, under experimentally verifiable assumptions, converge to a statistical solution.

The research presented here is based on the author's work in Parés-Pulido (2021).

2 Statistical solutions of the incompressible Euler equations

2.1 Correlation measures

Let us employ the following notation: for a finite, signed Radon measure $\mu \in \mathcal{M}(\mathbb{R}^d)$, and a continuous function $f \in C(\mathbb{R}^d)$, we denote

$$\langle \mu, g(\xi) \rangle := \int_{\mathbb{R}^d} g(\xi) \, d\mu(\xi).$$

Throughout, we implicitly assume that $\xi \in \mathbb{R}^d$ is the argument of g, in order to write expressions like $\langle \mu, \xi \otimes \xi \rangle$ (rather than $\langle \mu, \mathrm{id} \otimes \mathrm{id} \rangle$). For a metrized set Ω with the implicit σ-algebra of Borel's sets, we denote by $\mathrm{Prob}(\Omega)$ the set of all probability distributions defined on Ω.

Definition 2.1. A ***Young measure*** is a map $\nu \colon D \to \mathrm{Prob}(\mathbb{R}^k)$ which is measurable in the weak* topology; i.e., for any function $g \in C_0(\mathbb{R}^k)$, the map

$$x \mapsto \langle \nu_x, g \rangle$$

is Borel-measurable. We denote for convenience $\nu_x := \nu(x)$.

In the definitions below, we denote by $B_r(x) \subset D$ the ball of center x and radius r in Euclidean norm; and by $\fint$ the averaged integral, $\fint_A f(x) \, dx = \frac{1}{\mathcal{L}(A)} \int_A f(x) \, dx$, with $\mathcal{L}$ the Lebesgue measure.

Definition 2.2. (Fjordholm, Lanthaler, Mishra, Fjordholm, Lanthaler & Mishra (2017))

A ***correlation measure*** is a collection $\boldsymbol{\nu} = (\nu^1, \nu^2, \dots)$ of maps, with $\nu^k \colon D^k \to \mathrm{Prob}\left((\mathbb{R}^d)^k\right)$ satisfying the following properties:

1. *Weak* measurability:* For all $k \in \mathbb{N}$, the map $\nu^k \colon D^k \to \mathrm{Prob}\left((\mathbb{R}^d)^k\right)$ is weak* measurable; i.e. ν^k is a ***Young measure*** from D^k to $(\mathbb{R}^d)^k$.

2. L^p-*boundedness:* there exists $p \in [1, \infty)$ such that ν^1 is L^p-bounded, in the sense that

$$\int_D \langle \nu_x^1, \|\xi\|^p \rangle \, dx < \infty.$$

3. *Symmetry:* If σ is a permutation of $\{1, \dots, k\}$ and $f \in C_0(\mathbb{R}^k)$ then $\langle \nu_{\sigma(\boldsymbol{x})}^k, f(\sigma(\boldsymbol{\xi})) \rangle = \langle \nu_{\boldsymbol{x}}^k, f(\boldsymbol{\xi}) \rangle$ for a.e. $\boldsymbol{x} \in D^k$. Here, we denote $\sigma(\boldsymbol{x}) = \sigma(x_1, x_2, \dots, x_k) = (x_{\sigma_1}, x_{\sigma_2}, \dots, x_{\sigma_k})$.

4. *Consistency:* If $f \in C_0\left((\mathbb{R}^d)^k\right)$ is of the form $f(\xi_1, \dots, \xi_k) = g(\xi_1, \dots, \xi_{k-1})$ for some $g \in C_0((\mathbb{R}^d)^{k-1})$, then $\langle \nu_{x_1, \dots, x_k}^k, f \rangle = \langle \nu_{x_1, \dots, x_{k-1}}^{k-1}, g \rangle$ for almost every $(x_1, \dots, x_k) \in D^k$.

5. *Diagonal continuity:*

$$\lim_{r \to 0} \int_D \fint_{B_r(x)} \langle \nu_{x,y}^2, \|\xi_1 - \xi_2\|^2 \rangle \, dy \, dx = 0.$$

Each element ν^k is called a **correlation marginal**. We let $\mathcal{L}^p(D; \mathbb{R}^d)$ denote the **set of all correlation measures** from D to $\mathbb{R}^d$,

$$\mathcal{L}^p(D; \mathbb{R}^d) := \left\{ \boldsymbol{\nu} = (\nu^1, \nu^2, \dots), \ \nu^k \colon D^k \to \operatorname{Prob}\left(\left(\mathbb{R}^d\right)^k\right), \boldsymbol{\nu} \text{ is a corr. meas.}, \int_D \langle \nu_x^1, \|\xi\|^p \rangle \, dx < \infty \right\}$$

It is known, Fjordholm, Lanthaler & Mishra (2017), that correlation measures and probability measures in L^p can be uniquely identified, through the following **main theorem of correlation measures**:

Theorem 2.3. *(Fjordholm, Lanthaler & Mishra (2017), Theorem 2.7)*
For every correlation measure $\boldsymbol{\nu} \in \mathcal{L}^p(D; \mathbb{R}^d)$, there exists a unique probability measure $\mu \in \operatorname{Prob}(L^p(D, \mathbb{R}^d))$ satisfying

$$\int_{L^p(D;\mathbb{R}^d)} \|\boldsymbol{u}\|_{L^p(D;\mathbb{R}^d)}^p \, d\mu(\boldsymbol{u}) < \infty, \tag{2.1}$$

such that $\forall k \in \mathbb{N}$, and $\forall g \in L^1\left(D^k; C_0\left(\left(\mathbb{R}^d\right)^k\right)\right)$,

$$\int_{D^k} \int_{(\mathbb{R}^d)^k} g(\boldsymbol{x}, \boldsymbol{\xi}) d\nu_x^k(\boldsymbol{\xi}) \, d\boldsymbol{x} = \int_{L^p(D,\mathbb{R}^d)} \int_{D^k} g(\boldsymbol{x}, \boldsymbol{u}(\boldsymbol{x})) \, d\boldsymbol{x} d\mu(\boldsymbol{u}), \tag{2.2}$$

where $\boldsymbol{u}(\boldsymbol{x})$ denotes the vector $(\boldsymbol{u}(x_1), \boldsymbol{u}(x_2), \dots, \boldsymbol{u}(x_k))$, and $g(\boldsymbol{x}, \boldsymbol{\xi}) := g(\boldsymbol{x})(\boldsymbol{\xi})$. Conversely, for every probability measure $\mu \in \operatorname{Prob}(L^p(D, \mathbb{R}^d))$ with finite moment (2.1), there exists a unique correlation measure $\boldsymbol{\nu} \in \mathcal{L}^p(D; \mathbb{R}^d)$ satisfying (2.2).
Moreover, the (tensor-valued) moments

$$m^k(\boldsymbol{x}) := \langle \nu_{\boldsymbol{x}}^k, \, \xi_1 \otimes \xi_2 \otimes \cdots \otimes \xi_k \rangle$$

uniquely determine the correlation measure $\boldsymbol{\nu}$, and thus its associated μ.

2.2 Time-parameterized probability measures in function spaces

In this section we introduce the mathematical space in which we will seek solutions of the incompressible Euler equations: **time-parameterized correlation measures**; or equivalently, by Theorem 2.3, time-parameterized probability measures in L^2.

Fix $T \in [0, \infty)$. We denote $L_x^p := L^p(D; \mathbb{R}^d)$; and $L_t^q(\mathcal{X}) := L^q([0, T], \mathcal{X})$, for $\mathcal{X}$ a Banach space.

Definition 2.4. (Lanthaler et al. (2021))

1. Consider a time-parameterized probability measure $\mu \colon [0, T) \to \operatorname{Prob}(L_x^2)$, and denote $\mu_t := \mu(t)$. If for all $F \in C_b(L_x^2)$ (i.e. continuous and bounded), the mapping

$$t \mapsto \int_{L_x^2} F(\boldsymbol{u}) \, d\mu_t(\boldsymbol{u})$$

is measurable for a.e. $t \in [0,T)$, we say that μ is **weak* measurable**.

2. We denote by $L^1_t(\text{Prob})$ the space of weak* measurable, time-parameterized probability measures such that

$$\int_0^T \int_{L^2_x} \|\boldsymbol{u}\|_{L^2_x} \, d\mu_t(\boldsymbol{u}) dt < \infty.$$

3. A weak* measurable, time-parameterized probability measure μ is called **time-regular** if there exist a constant $L \in \mathbb{N}$ and a mapping $(s,t) \mapsto \pi_{s,t} \in \text{Prob}(L^2_x \times L^2_x)$ such that for a.e. $s, t \in [0,T)$:

   - The measure $\pi_{s,t}$ is a transport plan from μ_s to μ_t. That is: for all measurable $A \subset L^2_x$, it holds that $\pi_{s,t}(A \times L^2_x) = \mu_s(A)$ and $\pi_{s,t}(L^2_x \times A) = \mu_t(A)$.
   - There exists a constant $C > 0$ such that

$$\int_{L^2_x \times L^2_x} \|\boldsymbol{u} - \boldsymbol{v}\|_{H^{-L}_x} d\pi_{s,t}(\boldsymbol{u}, \boldsymbol{v}) \le C|t - s|. \tag{2.3}$$

4. A family of time-parameterized, time-regular probability measures $\{\mu^\Delta_t\}_{\Delta > 0}$ is **uniformly time-regular** if the constants L and C in point 3 can be chosen independently of Δ.

We conclude this subsection with the following two results, which will be of use in the sequel.

Lemma 2.5. *(Lanthaler et al. (2021), Proposition 2.2) Let $\mu^\Delta_t \in L^1_t(\text{Prob})$ be a family of uniformly time-regular probability measures, for $\Delta > 0$. Assume there exists $R > 0$ such that $\mu^\Delta_t(B_R(0)) = 1$ for all $\Delta > 0$ and a.e. $t \in [0,T)$, and $B_R(0)$ the ball of radius R and center 0 in L^2. If there exists $\mu_t \in L^1_t(\text{Prob})$ such that $\mu^\Delta_t \to \mu_t$, i.e.,*

$$\lim_{\Delta \to 0^+} \int_0^T W_1(\mu^\Delta_t, \mu_t) \, dt = 0,$$

then μ_t is time-regular, with the same time-regularity constants C, L as the family μ^Δ_t.

We recall that for a Banach space X, and $\rho, \sigma \in \text{Prob}(X)$, the 1-Wasserstein metric W_1 is defined as

$$W_1(\rho, \sigma) := \inf \int_{X \times X} \|\xi - \zeta\| \, d\pi(\xi, \zeta),$$

where the infimum is taken over all transport plans π between ρ and σ.

Theorem 2.6. *(Lanthaler et al. (2021), Theorem 2.4) Let $\{\mu^h_t\}_{h>0}$ be a family of uniformly time-regular, weak* measurable probability measures in $L^1_t(\text{Prob})$, and assume that there exists $R > 0$ such that*

$$\mu^h_t(B_R(0)) = 1, \qquad \forall h > 0, \forall t \in [0,T).$$

Let $\boldsymbol{\nu}^h_t = (\nu^{h,1}_t, \nu^{h,2}_t, \dots)$ denote the corresponding time-parameterized correlation measures. If there exists a map $\Upsilon \colon [0,\infty) \to [0,\infty)$ with $\lim_{r \to 0^+} \Upsilon(r) = 0$ such that for all $h > 0$,

$$S^2_r(\boldsymbol{\nu}^h, T)^2 := \int_0^T \int_D \fint_{B_r(x)} \langle \nu^{h,2}_{t;x,y}, \|\xi_1 - \xi_2\|^2 \rangle \, dy \, dx \, dt \le \Upsilon(r),$$

6

then there exist a subsequence $h_j \to 0$, $j \in \mathbb{N}$ and a time-parameterized probability measure $\mu_t \in L_t^1(\text{Prob})$ such that

$$\int_0^T W_1(\mu_t^{h_j}, \mu_t) \, dt \overset{j \to \infty}{\longrightarrow} 0. \tag{2.4}$$

Furthermore, if we denote $\boldsymbol{\nu}_t = (\nu_t^1, \nu_t^2, \dots)$ the time-parameterized correlation measure associated to the limit μ, the following properties are preserved:

I. L^2-bound: for a.e. $t \in [0, T)$,

$$\int_D \langle \nu_{t,x}^1, \|\xi\|^2 \rangle \, dx \leq R^2.$$

II. The two-point correlations satisfy

$$S_r^2(\boldsymbol{\nu}, T)^2 \leq \Upsilon(r).$$

III. We say that a function $g \in C([0, T) \times D^k \times (\mathbb{R}^d)^k)$, is an **admissible observable** if there exists $C > 0$ such that for all $t \in [0, T)$, $\boldsymbol{x} \in D^k$, $\boldsymbol{\xi}, \boldsymbol{\xi}' \in (\mathbb{R}^d)^k$,

$$|g(t, \boldsymbol{x}, \boldsymbol{\xi})| \leq C \prod_{i=1}^k \left(1 + \|\xi_i\|^2\right),$$

$$|g(t, \boldsymbol{x}, \boldsymbol{\xi}) - g(t, \boldsymbol{x}, \boldsymbol{\xi}')| \leq C \sum_{i=1}^k L_i(\boldsymbol{\xi}, \boldsymbol{\xi}') \|\xi_i - \xi_i'\| \sqrt{1 + \|\xi_i\|^2 + \|\xi_i'\|^2},$$

with

$$L_i(\boldsymbol{\xi}, \boldsymbol{\xi}') := \prod_{j=1, j \neq i}^k \left(1 + \|\xi_i\|^2 + \|\xi_i'\|^2\right).$$

Then, any admissible observable g converges strongly in $L^1([0, T) \times D^k)$ in expectation, i.e.,

$$\lim_{j \to \infty} \int_0^T \int_{D^k} \left| \langle \nu_{t,\boldsymbol{x}}^{h_j, k}, g(t, \boldsymbol{x}, \xi) \rangle - \langle \nu_{t,\boldsymbol{x}}^k, g(t, \boldsymbol{x}, \xi) \rangle \right| \, d\boldsymbol{x} dt = 0.$$

2.3 Statistical solutions of the incompressible Euler equations

With the tools presented before, we can finally rigorously define the object of interest of this work: **statistical solutions** of the incompressible Euler equations. We follow notation here from Fjordholm, Lanthaler & Mishra (2017), Lanthaler et al. (2021).

Definition 2.7. (Lanthaler et al. (2021), Def. 3.1) A time-parameterized probability measure $\mu_t \in L_t^1(\text{Prob})$ is a **statistical solution of the incompressible Euler equations** with initial data $\bar{\mu} \in \text{Prob}(L^2(D; \mathbb{R}^d))$ if $t \mapsto \mu_t$ is time-regular, and the associated correlation measure $\boldsymbol{\nu}_t$ (in the sense of Theorem 2.3) satisfies:

1. Given $\phi_1, \dots, \phi_k \in C^\infty([0, T) \times D; \mathbb{R}^d)$ with $\text{div}(\phi_i) = 0$ for all $i = 1, \dots, k$, set

$$\phi(t, \boldsymbol{x}) = \phi_1(t, x_1) \otimes \cdots \otimes \phi_k(t, x_k), \quad \text{where } \boldsymbol{x} = (x_1, \dots, x_k) \in D^k.$$

7

Then $\nu^k = \nu^k_{t,x_1,\ldots,x_k}$ satisfies

$$\int_0^T \int_{D^k} \langle \nu^k, \xi_1 \otimes \cdots \otimes \xi_k \rangle : \partial_t \phi + \sum_{i=1}^k \langle \nu^k, \xi_1 \otimes \cdots \otimes F(\xi_i) \otimes \cdots \otimes \xi_k \rangle : \nabla_{x_i} \phi \, d\boldsymbol{x} \, dt$$
$$+ \int_{D^k} \langle \bar{\nu}^k, \xi_1 \otimes \cdots \otimes \xi_k \rangle : \phi(0, \boldsymbol{x}) \, d\boldsymbol{x} = 0. \tag{2.5}$$

Here $\bar{\nu}$ is the correlation measure corresponding to the initial data $\bar{\mu}$. We denote $F(\xi) := \xi \otimes \xi$ and the contraction in the second term is more explicitly given by

$$(\xi_1 \otimes \cdots \otimes F(\xi_i) \otimes \cdots \otimes \xi_k) : \nabla_{x_i} \phi = \left[\prod_{j \neq i} (\xi_j \cdot \phi_j) \right] (\xi_i \cdot \nabla_{x_i} \phi_i) \cdot \xi_i.$$

2. For all $\psi \in C_c^\infty(D)$, and for a.e. $\in [0, T)$,

$$\int_{D^2} \langle \nu^2_{t,x,y}, \xi_1 \otimes \xi_2 \rangle : (\nabla \psi(x) \otimes \nabla \psi(y)) \, dx \, dy = 0. \tag{2.6}$$

As is the case for weak solutions (cf. Lions' notion of dissipative solutions, Lions (1996)), a stronger definition of solution, including a condition on energy dissipation, provides better theoretical properties. This is the object of the following:

Definition 2.8. (Lanthaler et al. (2021), Def. 3.2) A statistical solution $\mu_t \in L_t^1(\text{Prob})$ of the incompressible Euler equations with initial data $\bar{\mu} \in \text{Prob}(L_x^2)$ is called a **dissipative statistical solution** if, for all $M \in \mathbb{N}$, for every choice of coefficients $\boldsymbol{\alpha} = (\alpha_i)_{i=1}^M \in (0, 1]$ with $\sum_{i=1}^M \alpha_i = 1$, and for every $(\bar{\mu}_1, \ldots, \bar{\mu}_M) \in \text{Prob}(L_x^2)^M$ with $\sum_{i=1}^M \alpha_i \bar{\mu}_i = \bar{\mu}$, there exists a function $t \mapsto (\mu_{1,t}, \ldots, \mu_{M,t})$ with $\sum_{i=1}^M \alpha_i \mu_i = \mu$ such that, for all $i \in \{1, \ldots, M\}$:

- $t \mapsto \mu_{i,t}$ is weak* measurable, with $\mu_{i,t}|_{t=0} = \bar{\mu}_i$;

- for all $\phi \in C_c^\infty([0, T) \times D)$ with $\text{div}(\phi) \equiv 0$,

$$\int_0^T \int_{L_x^2} \int_D [\boldsymbol{u} \cdot \partial_t \phi + (\boldsymbol{u} \otimes \boldsymbol{u}) : \nabla \phi] \, dx \, d\mu_{i,t}(\boldsymbol{u}) \, dt = - \int_{L_x^2} \int_D \boldsymbol{u} \cdot \phi(0, x) \, dx \, d\bar{\mu}_i(\boldsymbol{u});$$

- for a.e. $t \in [0, T)$, and for $i \in \{1, \ldots, M\}$,

$$\int_{L_x^2} \|\boldsymbol{u}\|_{L_x^2}^2 \, d\mu_{i,t}(\boldsymbol{u}) \leq \int_{L_x^2} \|\boldsymbol{u}\|_{L_x^2}^2 \, d\bar{\mu}_i(\boldsymbol{u}).$$

Dissipative statistical solutions are a recently derived framework, for which the currently available results appear promising. Specifically, the two following results are proven in Lanthaler et al. (2021). The first is that, under a regularity condition, dissipative statistical solutions satisfy short-time existence and uniqueness:

Theorem 2.9. *(Lanthaler et al. (2021), Corollary 3.1) If $s \geq \lfloor d/2 \rfloor + 2$, and if $\exists C > 0$ such that the initial data $\bar{\mu} \in \mathrm{Prob}(L_x^2)$ is concentrated on*

$$\{\bar{u} \in H^s(D; \mathbb{R}^d) \colon \|\bar{u}\|_{H^s(D;\mathbb{R}^d)} \leq C\},$$

then there exists $T^* > 0$, depending only on C, and a statistical solution $\mu_t \colon [0, T^*] \to \mathrm{Prob}(L_x^2)$ with initial data $\bar{\mu}$. Furthermore, μ_t is unique in the class of dissipative statistical solutions for $t \in [0, T^*]$.

The second result is that restricting to two dimensions, and under smoothness conditions, dissipative statistical solutions verify global existence and weak-strong uniqueness in the following sense:

Theorem 2.10. *(Lanthaler et al. (2021), Corollary 3.2) Let $d = 2$, and let $\alpha \in (0, 1)$. If $\bar{\mu}$ is concentrated on $C^{1,\alpha}(D; \mathbb{R}^d)$, and if there exists $M > 0$ such that $\bar{\mu}(B_M(0)) = 1$, then there exists a dissipative statistical solution μ_t with initial data $\bar{\mu}$. Furthermore, μ_t is unique in the class of dissipative statistical solutions with initial data $\bar{\mu}$.*

3   A deterministic finite volume scheme for the incompressible Euler equations

In this section we will present a numerical scheme for the incompressible Euler equations, originally presented in Leonardi (2018b), and based on the work of Bell et al. (1989). This is an efficient finite volume method based on a discrete Leray projection.

Let $\boldsymbol{e}_m$ be the m-th unit vector in the canonical basis of $\mathbb{R}^d$, $(\boldsymbol{e}_m)_i = \delta_{i,m}$. We assume a partition of D into a uniform Cartesian grid, with

$$O(\Delta x_1) = O(\Delta x_2) = \cdots = O(\Delta x_d) = O(h).$$

Let the set of cells be $\{C_{\boldsymbol{i}}\}_{\boldsymbol{i} \in I}$, with $C_{\boldsymbol{i}} := \prod_{m=1}^d [i_m \Delta x_m, (i_m + 1)\Delta x_m]$, for $\boldsymbol{i} = (i_1, \ldots, i_d) \in I$ the set of indices in the Cartesian mesh, $I = \{1, \ldots, N_1\} \times \cdots \times \{1, \ldots, N_d\}$. We refer by $x_{\boldsymbol{i}}$ to the midpoint of cell $C_{\boldsymbol{i}}$. We term $\mathcal{G}_h$ the set of piecewise constant functions in the grid, i.e.,

$$\mathcal{G}_h^k := \{\boldsymbol{u} \colon D \to \mathbb{R}^k \colon \boldsymbol{u}\big|_{\mathring{C}_{\boldsymbol{i}}} \text{ constant } \forall \boldsymbol{i} \in I\}.$$

We implicitly identify a function in $\mathcal{G}_h^k$ with the vector of cell averages in $\mathbb{R}^{k|I|}$; e.g. for $\boldsymbol{u} \in \mathcal{G}_h^k$, we write $\|\boldsymbol{u}\|_{L^2(D)}^2 = \sum_{\boldsymbol{i} \in I} \|\boldsymbol{u}_{\boldsymbol{i}}\|_2^2 \Delta x_1 \cdots \Delta x_d$.

For $\boldsymbol{u} = (u_1, \ldots, u_d) \in \mathcal{G}_h^d$ (i.e. $u_i \in \mathcal{G}_h^1$ for all i), and $\varphi \in \mathcal{G}_h^1$, we define the following operators:

$$\mathrm{div}^h \colon \mathcal{G}_h^d \to \mathcal{G}_h^1; \qquad (\mathrm{div}^h \boldsymbol{u})_{\boldsymbol{i}} := \sum_{m=1}^d \frac{(u_m)_{\boldsymbol{i}+\boldsymbol{e}_m} - (u_m)_{\boldsymbol{i}-\boldsymbol{e}_m}}{2\Delta x_m},$$

$$\mathrm{grad}^h \colon \mathcal{G}_h^1 \to \mathcal{G}_h^d; \qquad (\mathrm{grad}^h \varphi)_{\boldsymbol{i}} := \left[\frac{\varphi_{\boldsymbol{i}+\boldsymbol{e}_1} - \varphi_{\boldsymbol{i}-\boldsymbol{e}_1}}{2\Delta x_1}, \ldots, \frac{\varphi_{\boldsymbol{i}+\boldsymbol{e}_d} - \varphi_{\boldsymbol{i}-\boldsymbol{e}_d}}{2\Delta x_d} \right],$$

$$\Delta^h \colon \mathcal{G}_h^1 \to \mathcal{G}_h^1; \qquad (\Delta^h \varphi)_{\boldsymbol{i}} := \sum_{m=1}^d \frac{\varphi_{\boldsymbol{i}+2\boldsymbol{e}_m} - 2\varphi_{\boldsymbol{i}} + \varphi_{\boldsymbol{i}-2\boldsymbol{e}_m}}{4\Delta x_m^2}.$$

We will denote by $\mathcal{G}_h^{d,div}$ the vector subspace in $\mathcal{G}_h^d$ of discretely divergence-free functions, i.e.

$$\mathcal{G}_h^{d,div} = \{\boldsymbol{u} \in \mathcal{G}_h^d \colon \operatorname{div}^h \boldsymbol{u} \equiv 0\}.$$

Recall that we will assume for convenience periodic boundaries. A first trivial observation:

Lemma 3.1. *Let* $\boldsymbol{u} \in \mathcal{G}_h^d$, $\psi \in \mathcal{G}_h^1$. *Then it holds that:*

$$\sum_{\boldsymbol{i} \in I} \boldsymbol{u_i} \cdot \operatorname{grad}^h \psi_{\boldsymbol{i}} = -\sum_{\boldsymbol{i} \in I} \psi_{\boldsymbol{i}} \operatorname{div}^h \boldsymbol{u_i}.$$

With this notation, we are finally in position of defining the finite volume scheme of Leonardi (2018*b*). Fix $\theta \in \left(\frac{1}{2}, 1\right]$. The scheme has the following form; a detailed explanation of each operator therein follows.

$$\frac{\boldsymbol{u}^{*,n+1} - \boldsymbol{u}^n}{\Delta t^n} + \boldsymbol{C}(\boldsymbol{u}^n, \widetilde{\boldsymbol{u}}^{n+\frac{1}{2}}) = \boldsymbol{D}(\widetilde{\boldsymbol{u}}^{n+\frac{1}{2}}) \tag{3.1}$$

$$\frac{\boldsymbol{u}^{n+1} - \boldsymbol{u}^n}{\Delta t^n} = \boldsymbol{P}^h \left(\frac{\boldsymbol{u}^{*,n+1} - \boldsymbol{u}^n}{\Delta t^n} \right), \tag{3.2}$$

coupled with the initial condition $\boldsymbol{u}^0 = \Pi_h^{div}(\overline{\boldsymbol{u}}) \in \mathcal{G}_h^{d,div}$, and with time-averaged velocity $\widetilde{\boldsymbol{u}}^{n+\frac{1}{2}} \in \mathcal{G}_h^d$ defined as

$$\widetilde{\boldsymbol{u}}^{n+\frac{1}{2}} := \theta \boldsymbol{u}^{*,n+1} + (1-\theta)\boldsymbol{u}^n.$$

In the scheme above, the operators are defined as follows:

- Operator $\boldsymbol{C}$ approximates the convective term $[(\boldsymbol{u} \cdot \nabla)\boldsymbol{u}]$ as

$$\boldsymbol{C} \colon \mathcal{G}_h^d \times \mathcal{G}_h^d \to \mathcal{G}_h^d$$

$$\boldsymbol{C}(\boldsymbol{u}, \boldsymbol{v})_{\boldsymbol{i}} = \sum_{m=1}^{d} \frac{\boldsymbol{F}^m(\boldsymbol{u_i}, \boldsymbol{u_{i+e_m}}, \boldsymbol{v_i}, \boldsymbol{v_{i+e_m}}) - \boldsymbol{F}^m(\boldsymbol{u_{i-e_m}}, \boldsymbol{u_i}, \boldsymbol{v_{i-e_m}}, \boldsymbol{v_i})}{\Delta x_m}$$

with, denoting $\boldsymbol{u}^L := (u_i^L)_{i=1}^d$, and analogously for $\boldsymbol{u}^R$:

$$\boldsymbol{F}^m \colon \mathcal{G}_h^d \times \mathcal{G}_h^d \times \mathcal{G}_h^d \times \mathcal{G}_h^d \longrightarrow \mathcal{G}_h^d$$

$$\boldsymbol{F}^m(\boldsymbol{u}^L, \boldsymbol{u}^R, \boldsymbol{v}^L, \boldsymbol{v}^R) = \frac{u_m^L + u_m^R}{4}(\boldsymbol{v}^L + \boldsymbol{v}^R).$$

- Operator $\boldsymbol{D}$ is a Lax-Wendroff second order diffusion operator,

$$\boldsymbol{D} \colon \mathcal{G}_h^d \to \mathcal{G}_h^d$$

$$\boldsymbol{D}(\boldsymbol{u})_{\boldsymbol{i}} = \epsilon \sum_{m=1}^{d} \frac{\|[\![\boldsymbol{u}]\!]_{\boldsymbol{i},m}\|_2 [\![\boldsymbol{u}]\!]_{\boldsymbol{i},m} - \|[\![\boldsymbol{u}]\!]_{\boldsymbol{i}-\boldsymbol{e}_m,m}\|_2 [\![\boldsymbol{u}]\!]_{\boldsymbol{i}-\boldsymbol{e}_m,m}}{\Delta x_m},$$

with $\epsilon > 0$ fixed, and $[\![\boldsymbol{u}]\!]_{\boldsymbol{i},m} := \boldsymbol{u_{i+e_m}} - \boldsymbol{u_i}$.

- Operator $\boldsymbol{P}^h$ is a discretely divergence-free projection, given by

$$\boldsymbol{P}^h \colon \mathcal{G}_h^d \to \mathcal{G}_h^{d,div}$$
$$\boldsymbol{P}^h(\boldsymbol{u}) = \boldsymbol{u} - \operatorname{grad}^h \psi,$$

where $\psi(\equiv \psi(\boldsymbol{u})) \in \mathcal{G}_h^1$ is the solution of the linear system of equations

$$\Delta^h \psi = \operatorname{div}^h \boldsymbol{u},$$

paired with suitable boundary conditions. It is not difficult to see, cf. Lemma 3.22, Parés-Pulido (2021), that this is indeed a well-defined, orthogonal projection operator, which acts as a linear transformation of $\boldsymbol{u}$.

- For $h > 0$, and for $p \geq 1$, let $A^h \colon L^p(D)^d \to \mathcal{G}_h^d$ be the **cell averaging operator**, given by $\left(A^h(\phi)\right)_{\boldsymbol{i}} := \fint_{C_{\boldsymbol{i}}} \phi(\boldsymbol{x}) \, d\boldsymbol{x}$. Let $\Pi_h^{div} \colon L^2(D; \mathbb{R}^d) \to \mathcal{G}_h^{d,div}$ be defined by

$$\Pi_h^{div} \equiv \boldsymbol{P}^h \circ A^h.$$

We now list some elementary properties of scheme (3.1)-(3.2). Proofs are omitted for brevity, but they are straightforward with standard techniques; they can all be found in Parés-Pulido (2021).

Lemma 3.2. *Assume there exists $\lambda > 0$, independent of h, with $\Delta t^n < \lambda h \; \forall n$. Then*

I. *Projection operator $\boldsymbol{P}^h$ is energy-dissipative, i.e. for all $\boldsymbol{u}^* \in \mathcal{G}_h^d$,*

$$\|\boldsymbol{P}^h(\boldsymbol{u}_{\boldsymbol{i}}^*)\|_{L^2} \leq \|\boldsymbol{u}_{\boldsymbol{i}}^*\|_{L^2}.$$

II. *Scheme (3.1)-(3.2) is **energy-stable** or L^2-stable; i.e.,*

$$\|\boldsymbol{u}_{\boldsymbol{i}}^{n+1}\|_{L^2} \leq \|\boldsymbol{u}_{\boldsymbol{i}}^n\|_{L^2}.$$

III. *For all $m \in \{1, 2, \ldots, d\}$, scheme (3.1)-(3.2) satisfies:*

$$\sum_{n=0}^{N-1} \sum_{\boldsymbol{i} \in I} \|\widetilde{\boldsymbol{u}}_{\boldsymbol{i}+\boldsymbol{e}_m}^{n+\frac{1}{2}} - \widetilde{\boldsymbol{u}}_{\boldsymbol{i}}^{n+\frac{1}{2}}\|_2^3 \Delta x_1 \cdots \Delta x_d \Delta t^n \leq C \|\boldsymbol{u}^0\|_{L^2(D)}^2 h,$$

$$\sum_{n=0}^{N-1} \sum_{\boldsymbol{i} \in I} \|\boldsymbol{u}^{*;n+1}_{\boldsymbol{i}} - \boldsymbol{u}_{\boldsymbol{i}}^n\|_2^2 \Delta x_1 \cdots \Delta x_d \Delta t^n \leq C \|\boldsymbol{u}^0\|_{L^2(D)}^2 h,$$

with C independent of $\boldsymbol{u}$ and h.

IV. *Scheme (3.1)-(3.2) is **total-variation vanishing**, in the following sense:*

$$\sum_{m=1}^{d} \sum_{n=0}^{N-1} \sum_{\boldsymbol{i} \in I} \left\|\boldsymbol{u}_{\boldsymbol{i}+\boldsymbol{e}_m}^n - \boldsymbol{u}_{\boldsymbol{i}}^n\right\|_2^2 \Delta x_1 \ldots \Delta x_d \Delta t^n \leq C \|\boldsymbol{u}^0\|_{L^2(D)}^{\frac{4}{3}} h^{\frac{2}{3}},$$

11

where C is independent of $\boldsymbol{u}$ and h.

V. *Operator $\boldsymbol{D}$ (weakly) vanishes in the limit. That is: for all $\phi \in C^\infty([0,T] \times D; \mathbb{R}^d)$ such that for a.e. $t \in [0,T)$, $\mathrm{div}(t,\cdot) \equiv 0$, let $\phi^h(t,\cdot) := \Pi_h^{div} \circ \phi(t,\cdot)$. Then there exists $C > 0$ independent of ϕ, $\boldsymbol{u}$ and h such that*

$$\left| \int_0^T \int_D \boldsymbol{D}(\widetilde{\boldsymbol{u}}(t,x)) \cdot \phi^h(t,x) \, dx \, dt \right| \le C \|\boldsymbol{u}_0\|_{L^2(D)}^{\frac{4}{3}} h^{\frac{2}{3}}.$$

Additionally the following properties are useful for the main results of this work in the sequel. Their proofs are fairly technical; we refer the interested reader to Appendix A in Parés-Pulido (2021).

Lemma 3.3. *Projection operator $\Pi_h^{div} \colon L^2(D; \mathbb{R}^d) \to \mathcal{G}_h^{d,div}$ satisfies the following properties:*

I. *Let $\phi \in C^2(D; \mathbb{R}^d)$ with $\mathrm{div}(\phi) \equiv 0$. There exists $C = C\left(\max\limits_{|\alpha|=2} |D^\alpha \phi| \right) > 0$ such that*

$$\|\phi - \Pi_h^{div} \circ \phi\|_{L^2(D;\mathbb{R}^d)} \le Ch.$$

II. *There exists $C(d)$ such that for all $\phi \in L^2(D; \mathbb{R}^d)$, and for all $h > 0$,*

$$\|\Pi_h^{div}(\phi)\|_{L^2(D;\mathbb{R}^d)} \le C(d) \|\phi\|_{L^2(D;\mathbb{R}^d)}.$$

III. *If $\phi \in C^2(D; \mathbb{R}^d)$ has $\mathrm{div}(\phi) \equiv 0$, and $\phi^h := \Pi_h^{div}(\phi)$, then*

$$\lim_{h \to 0^+} \max_{\boldsymbol{i} \in I} \|\phi_{\boldsymbol{i}}^h - \phi(x_{\boldsymbol{i}})\|_\infty = 0,$$

$$\lim_{h \to 0^+} \max_{\boldsymbol{i} \in I} \left\| \frac{\phi_{\boldsymbol{i}+\boldsymbol{e}_m}^h - \phi_{\boldsymbol{i}}^h}{h} - \partial_{x_m} \phi(x_{\boldsymbol{i}}) \right\|_\infty = 0.$$

IV. *Π_h^{div} preserves time-regularity. That is, if $\phi \in L^\infty([0,T] \times D, \mathbb{R}^d)$ is such that $\phi(\cdot, x) \in C^1([0,T], \mathbb{R}^d)$ for a.e. x, then the function $\tilde{\phi}(t,\cdot) := \Pi_h^{div} \circ \phi(t,\cdot)$ also has $\tilde{\phi}(\cdot, x) \in C^1([0,T], \mathbb{R}^d)$ for all x.*

4 A convergent finite volume scheme for statistical solutions of the incompressible Euler equations

In this section, we present the main results of this work. We introduce a Monte Carlo scheme, built upon the deterministic finite volume scheme presented in the previous section; and we rigorously show that it converges to a statistical solution. This convergence is only under an external assumption; in Section 5 we will show numerical evidence that this hypothesis is mild for cases of practical interest.

The Monte Carlo scheme is based on the well-known concept of **_ensemble simulations_**. Although it has long been present in the literature, especially for numerical weather forecasting, e.g. (Epstein (1969), Leith (01 Jun. 1974)), we follow the more recent presentation in Fjordholm, Käppeli, Mishra & Tadmor (2017) of an analogous method for hyperbolic conservation laws.

The specific formulation of the scheme that we follow is that of Leonardi (2018a,b); we also employ the numerical solver of the same author, Leonardi (2017a). In the original presentation, the scheme is considered as an approximation method for measure-valued solutions. In this work, we prove that the scheme contains, in fact, sufficient information to converge to a statistical solution.

Throughout this section, we consider the initial value problem for the incompressible Euler equations in the sense of **uncertainty quantification**: we consider initial data randomly distributed according to a probability measure $\bar{\mu} \in L^2(D; \mathbb{R}^d)$. For a deterministic initial condition, we will adopt the same approach as e.g. Fjordholm et al. (2016) and introduce an arbitrary, small random perturbation to the initial datum, and thus view it as a probability measure; we will discuss this in more detail in Section 5.

4.1 Notation

Let $L_{div}^p(D) \subset L^p(D; \mathbb{R}^d)$ be the space of weakly divergence-free functions in L^p, i.e.

$$L_{div}^p(D; \mathbb{R}^d) := \left\{ \boldsymbol{u} \in L^p(D; \mathbb{R}^d) : \int_D \boldsymbol{u} \cdot \nabla F = 0, \ \forall F \in C^\infty(D; \mathbb{R}) \right\}.$$

For simplicity of the exposition, we will henceforth assume a uniform Cartesian mesh in all directions, i.e., for all $m \in \{1, \dots, d\}$ and $\boldsymbol{i} \in I$, $x_{\boldsymbol{i}+\boldsymbol{e}_m} - x_{\boldsymbol{i}} =: h$. Let $\overline{\boldsymbol{u}} \in L_{div}^2(D)$. For $h > 0$, let

$$\boldsymbol{u}^{h;0} := \Pi_h^{div} \circ \overline{\boldsymbol{u}} \in \mathcal{G}_h^{d,div}$$

and for all $n \in \{1, \dots, N\}$, let $\boldsymbol{u}^{h;n}$ be obtained with algorithm (3.1)-(3.2) with $\boldsymbol{u}^{h;0}$ as initial datum. Thus we can define the following piecewise linear in time evolution operator:

$$
\begin{aligned}
\mathcal{S}^h &: [0,T] \times L_{div}^2(D) \to \mathcal{G}_h^{d,div} \cap L^2(D; \mathbb{R}^d) \\
\mathcal{S}^h(t, \overline{\boldsymbol{u}})(\cdot) &:= \sum_{n=0}^{N(h)-1} \left(\frac{t^{n+1}-t}{\Delta t^n} \boldsymbol{u}^{h;n}(\cdot) + \frac{t-t^n}{\Delta t^n} \boldsymbol{u}^{h;n+1}(\cdot) \right) \chi_{[t^n, t^{n+1})}(t).
\end{aligned}
\tag{4.1}
$$

For brevity we write $\mathcal{S}_t^h \overline{\boldsymbol{u}} := \mathcal{S}^h(t, \overline{\boldsymbol{u}})$. Given an initial distribution $\bar{\mu} \in \text{Prob}(L_{div}^2(D; \mathbb{R}^d))$, for all $t \in [0,T]$ we can define a probability measure in $L^2(D; \mathbb{R}^d)$ at time t, via push-forward measure:

$$\mu_t^h := \mathcal{S}_t^h \# \bar{\mu}. \tag{4.2}$$

4.2 The Monte Carlo algorithm

We can now present the numerical algorithm that we will use in this work, which follows the FKMT algorithm in Lye (2020), Fjordholm, Käppeli, Mishra & Tadmor (2017).

Algorithm 4.1. (FKMT algorithm for the incompressible Euler equations).
Let $\bar{\mu} \in \text{Prob}(L^2(D; \mathbb{R}^d))$; and for a mesh width $h > 0$, let $\mathcal{S}^h$ be the evolution operator as in (4.1). Fix a number of samples M.

1. Generate $\overline{\boldsymbol{u}}_1, \overline{\boldsymbol{u}}_2, \dots, \overline{\boldsymbol{u}}_M \in L^2(D; \mathbb{R}^d)$ independent random variables with distribution $\bar{\mu}$.

2. For $m \in \{1, \dots, M\}$, evolve the sample in time, $\boldsymbol{u}_m^h(t) := \mathcal{S}_t^h(\overline{\boldsymbol{u}}_m)$.

3. Estimate the statistical solution by the **empirical measure**

$$\mu_t^{h,M} := \frac{1}{M} \sum_{m=1}^{M} \delta_{\boldsymbol{u}_m^h(\cdot,t)}.$$

4.3   Convergence of the initial data

Lemma 4.2. *Let $\mu \in \mathrm{Prob}(L^2(D;\mathbb{R}^d))$ with $\boldsymbol{u} \in L^2_{div}$ μ-almost surely. For $h > 0$, define $\mu^h := \Pi_h^{div}\#\mu$. For all $G \in C^1(D \times \mathbb{R}^d; \mathbb{R}^k)$,*

$$\lim_{h \to 0} \left\| \int_{L^2(D;\mathbb{R}^k)} \int_D G(x, \boldsymbol{u}(x))\, dx\, d\mu(\boldsymbol{u}) - \int_{L^2(D;\mathbb{R}^k)} \int_D G(x, \boldsymbol{u}(x))\, dx\, d\mu^h(\boldsymbol{u}) \right\|_2 = 0.$$

Proof. μ^h is well-defined, as Π_h^{div} is measurable by construction. Furthermore,

$$\left\| \int_{L^2(D;\mathbb{R}^k)} \int_D G(x, \boldsymbol{u}(x))\, dx\, d\mu(\boldsymbol{u}) - \int_{L^2(D;\mathbb{R}^k)} \int_D G(x, \boldsymbol{u}(x))\, dx\, d\mu^h(\boldsymbol{u}) \right\|_2$$

$$\leq (\mathcal{L}(D))^{\frac{1}{2}} \|\nabla_{\boldsymbol{u}} G\|_{L^\infty(D;\mathbb{R}^{k \times d})} \int_{L^2(D;\mathbb{R}^d)} \left\| \boldsymbol{u} - \Pi_h^{div} \circ \boldsymbol{u} \right\|_{L^2(D;\mathbb{R}^d)}\, d\mu(\boldsymbol{u}).$$

Through Lemma 3.3.I, μ-a.s., $\left\| \boldsymbol{u} - \Pi_h^{div} \circ \boldsymbol{u} \right\|_{L^2(D;\mathbb{R}^d)} \to 0$ as $h \to 0$, and the conclusion is immediate.
$\square$

4.4   Time-regularity

Lemma 4.3. *Let $\bar{\mu} \in \mathrm{Prob}(L^2(D;\mathbb{R}^d))$ with $\boldsymbol{u} \in L^2_{div}$ $\bar{\mu}$-a.s, and such that there exists $R > 0$ with $\mathrm{supp}(\bar{\mu}) \subset B_R(0)$, the ball of radius R and center 0 in $L^p(D;\mathbb{R}^d)$. Let $\{\mu^h\}_{h>0}$ be a family of time-parameterized probability measures generated by (4.2), and assume $\Delta t^n = O(h)$. Then this family is uniformly time-regular.*

Proof. Fix $h > 0$, and let $s, t \in [0, T]$ with $s < t$. As μ_t^h and μ_s^h are discrete distributions, trivially a transport map between the two exists.

We now verify that there exist constants $C > 0$, and $L \in \mathbb{N}$, independent of h, such that for any realization of the initial data $\bar{\mu}$, denoted by element ω,

$$\|\boldsymbol{u}(\omega; t, \cdot) - \boldsymbol{u}(\omega; s, \cdot)\|_{H_x^{-L}} \leq C|t - s|$$

which obviously implies eq. (2.3), $\int_{L_x^2 \times L_x^2} \|\boldsymbol{w} - \boldsymbol{v}\|_{H_x^{-L}} d\pi_{s,t}(\boldsymbol{w}, \boldsymbol{v}) \leq C|t - s|$.

We omit the parameter ω in the rest of this proof. Let $k \geq 2$ and let $\Phi \in H^k(D; \mathbb{R}^d)$. We will assume Φ is divergence-free in the sequel. If it is not, a straightforward argument of Helmholtz decomposition guarantees that the integral involving the gradient term is vanishingly small. For convenience, let us assume there exist $\tilde{n}, \tilde{m}$ such that $s = t^{\tilde{n}}$, $t = t^{\tilde{m}}$; the proof below only needs a minor, trivial modification

otherwise. Then

$$\left| \int_D \left(\boldsymbol{u}(x,t) - \boldsymbol{u}(x,s) \right) \cdot \Phi(x) \, dx \right| = \left| \sum_{n=\tilde{n}}^{\tilde{m}-1} \int_D \int_{t^n}^{t^{n+1}} \partial_t \boldsymbol{u}(x,\tau) \cdot \Phi(x) \, d\tau \, dx \right|.$$

For any time interval (t^n, t^{n+1}), $\partial_t \boldsymbol{u}$ is ($\bar{\mu}$-a.s.) well defined, and in fact has a constant value of $\frac{1}{\Delta t^n}(\boldsymbol{u}^{n+1} - \boldsymbol{u}^n)$. Therefore, by definition of the numerical scheme (3.1)-(3.2),

$$\int_D \int_{t^n}^{t^{n+1}} \partial_t \boldsymbol{u}(x,\tau) \cdot \Phi(x) \, d\tau = \Delta t^n \int_D \left[-\boldsymbol{C}^h(\boldsymbol{u}^n, \widetilde{\boldsymbol{u}}^{n+\frac{1}{2}}) + \boldsymbol{D}^h(\widetilde{\boldsymbol{u}}^{n+\frac{1}{2}}) - \operatorname{grad}^h \psi^{h;n} \right] \cdot \Phi(x) \, dx$$

Due to the density of smooth functions in H^2, we can assume $\Phi \in C^\infty$; otherwise the difference can be made arbitrarily small, and the L^2 bound in Lemma 3.3.III allows one to disregard it. Furthermore, if Φ is smooth, the difference between its cell averages $\bar{\Phi}$ and Φ vanishes uniformly as $h \to 0$; and as Φ is divergence-free, 3.3.I gives that $\|\Phi - \Pi_h^{div} \circ \Phi\|_{L^2}$ also vanishes uniformly.

With an easy argument based on the Lipschitz-continuity of the fluxes $\boldsymbol{F}^m$ in $\boldsymbol{C}$, $\int_D \boldsymbol{C}^h(\boldsymbol{u}^n, \widetilde{\boldsymbol{u}}^{n+\frac{1}{2}}) \cdot \bar{\Phi}(x) \, dx$ can be bounded, up to an additive error term that vanishes as $h \to 0$, by a term of the form

$$\sum_{\boldsymbol{i} \in I} h^d \sum_{m=1}^d (u_{\boldsymbol{i}}^n)_m \boldsymbol{u}_{\boldsymbol{i}}^n \cdot \frac{\bar{\Phi}_{\boldsymbol{i}+\boldsymbol{e}_m} - \bar{\Phi}_{\boldsymbol{i}}}{h}$$

which in turn can be bounded by $\|\boldsymbol{u}^n\|_{L^2}^2 \|\nabla\Phi\|_{L^\infty}$ by smoothness of Φ.

An analogous idea (cf. Lemma 3.2.V) lets us transfer one discrete derivative from $\boldsymbol{D}^h$ to $\bar{\Phi}$, obtaining a similar bound of the type $\|\boldsymbol{u}^n\|_{L^2} \|\nabla\Phi\|_{L^\infty}$ for the term $\int_D \boldsymbol{D}^h(\widetilde{\boldsymbol{u}}^{n+\frac{1}{2}}) \cdot \Phi(x) \, dx$. The term $\int_D \operatorname{grad}^h \psi^{h;n} \cdot \Phi^h(x) \, dx$ is identically zero through Lemma 3.1.

Now, choosing $2 \le L \in \mathbb{N}$ large enough that, by Sobolev's inequality, $H^L(D; \mathbb{R}^d)$ continuously embeds in $W^{1,\infty}(D; \mathbb{R}^d)$, we can bound the L^∞ norms above by Sobolev norms. As $\|\boldsymbol{u}\|_{L^2} \le R$, then, we can conclude that

$$\left| \int_D \left(\boldsymbol{u}(x,t) - \boldsymbol{u}(x,s) \right) \cdot \Phi(x) \, dx \right| \le C'(d)(t-s)R^2 \|\Phi\|_{H^L},$$

and thus

$$\|\boldsymbol{u}(\omega; t, \cdot) - \boldsymbol{u}(\omega; s, \cdot)\|_{H_x^{-L}} \le R^2 C'(d)|t-s|.$$

$\square$

Theorem 4.4. *Fix $p \in [1, \infty)$. Let $\bar{\mu} \in \operatorname{Prob}(L^p(D; \mathbb{R}^d))$ represent a set of stochastic initial data for the incompressible Euler equations, with $\boldsymbol{u} \in L_{div}^p$ $\bar{\mu}$-almost surely. Assume that there exists $R > 0$ with $\operatorname{supp}(\bar{\mu}) \subset B_R(0)$, the ball of radius R and center 0 in $L^p(D; \mathbb{R}^d)$. For $h > 0$, let $\mu_t^h = \mathcal{S}_t^h \# \mu$ as in eq. (4.2). Assume furthermore that the discrete projection scheme (3.1)-(3.2) satisfies the following properties:*

- L^p *bounds:* $\exists C > 0$ *such that*

$$h^d \sum_{\boldsymbol{i} \in I} \|\boldsymbol{u}_{\boldsymbol{i}}^{h;n}\|_2^p \leq C h^d \sum_{\boldsymbol{i} \in I} \|\boldsymbol{u}^{h;0}\|_2^p \tag{4.3}$$

for all $n \in \{0, 1, \dots, N\}$.

- *For all* $r \leq h$, *there exist* α, $C > 0$ *(independent of h) such that*

$$S_r^p(\mu^h, T) \leq C r^\alpha, \tag{4.4}$$

with $S_r^p(\mu, T)$ *the time-averaged structure function*

$$S_r^p(\mu, T) := \left(\int_0^T \int_{L^p(D;\mathbb{R}^d)} \int_D \fint_{B_r(x)} \|\boldsymbol{u}(x) - \boldsymbol{u}(y)\|_2^p \, dy \, dx \, d\mu_t(\boldsymbol{u}) \, dt \right)^{\frac{1}{p}}.$$

- *Scaling assumption: for all* $\ell > 1$, *there exist* $\bar{C} > 0$, $\beta \leq \alpha$ *(independent of h) such that*

$$S_{\ell r}^p(\mu^h, T) \leq \bar{C} \ell^\beta S_r^p(\mu^h, T). \tag{4.5}$$

Then there exists a subsequence $h' \to 0$ such that the approximate statistical solutions $\mu^{h'}$ converge strongly to some $\mu \in L_t^1(\text{Prob})$, in the sense of Theorem 2.6.

Proof. Let us verify that the conditions of Theorem 2.6 are met; hence a converging subsequence exists. Uniform time-regularity is immediate from Lemma 4.3.

Let $\{h_l\}_{l \in \mathbb{N}} \subset \mathbb{R}$, with $\{h_l\} \searrow 0$. Let us denote $\boldsymbol{\nu}_l = (\nu_l^1, \nu_l^2, \dots)$ the time-parameterized correlation measure associated with $\mu^{h_l} = \mathcal{S}_t^{h_l} \# \mu$ (in the sense of Theorem 2.3). L^p-boundedness is immediate: since $\text{supp}(\bar{\mu}) \subset B_R(0)$, we have

$$\sup_{l \to \infty} \sup_{t \in [0,T)} \int_D \langle \nu_{l;t,x}^1, \|\xi\|_2^p \rangle \, dx$$

$$= \sup_{l \to \infty} \max_{0 \leq n \leq N(l)} \int_{L^p(D;\mathbb{R}^d)} \sum_{\boldsymbol{i} \in I} h_l^d \|\boldsymbol{u}(x_{\boldsymbol{i}})\|_2^p \, d\mu_{t^n}^{h_l}(\boldsymbol{u})$$

$$\overset{(4.3)}{\leq} \sup_{l \to \infty} C \int_{L^p(D;\mathbb{R}^d)} \sum_{\boldsymbol{i} \in I} h_l^d \|\boldsymbol{u}(x_{\boldsymbol{i}})\|_2^p \, d\mu_0^{h_l}(\boldsymbol{u})$$

$$\leq \sup_{l \to \infty} C' \int_{L^p(D;\mathbb{R}^d)} \|\boldsymbol{u}\|_{L^p(D;\mathbb{R}^d)}^p \, d\bar{\mu}(\boldsymbol{u}) \leq C' R^p < \infty \tag{4.6}$$

where the inequality that begins line (4.6) is justified by Lemma 4.2, taking G to be the identity function.

For the second property in Theorem 2.6, we need to show that

$$\lim_{r \to 0} \limsup_{l \to \infty} \int_0^{T'} \int_D \fint_{B_r(x)} \langle \nu_{l;t,x,y}^2, \|\xi_1 - \xi_2\|^p \rangle \, dy \, dx \, dt = 0, \tag{4.7}$$

16

for all $T' \in [0, T)$. For $r \leq h_l$, from hypothesis (4.4), this is immediate. For $r > h_l$, choose $\ell > 1$ and $h < h_l$ such that $r = \ell h$.

$$S_r^p(\mu^{h_l}, T) = S_{\ell h}^p(\mu^{h_l}, T) \overset{(4.5)}{\leq} C \ell^\beta S_h^p(\mu^{h_l}, T) \overset{(4.4)}{\leq} C'' \ell^\beta h^\alpha \leq C''' r^\beta,$$

where the bound is independent of l. Hence, through claim (4.7), Theorem 2.6 guarantees convergence up to a subsequence to some time-parameterized correlation measure μ. $\qquad\square$

Remark 4.5. *Comparing with Lemma 3.2.II, hypothesis (4.3) holds (with $p = 2$) for scheme (3.1)-(3.2). Furthermore, it is not difficult to see, cf. Fjordholm et al. (2020), Theorem 4.1 or Parés-Pulido (2021), Theorem 4.4, that the total variation bound in Lemma 3.2.IV implies hypothesis (4.4).*

The scaling assumption (4.5) is considerably more difficult, and there is little expectation of being able to derive it. We remark that this assumption is a discrete version of the scaling hypothesis in Kolmogorov's K41 theory (see e.g. Chapter 6 in Frisch & Kolmogorov (1995)); which is a common assumption in turbulence models, widely considered to hold in practice. Thus, the hypothesis appears natural.

Remark 4.6. *If there exist $K > 0$ and $\gamma \in (0, 1]$ such that for all h,*

$$S_r^p(\mu^h, T) \leq K r^\gamma,$$

then assumption (4.4) holds with $\alpha := \gamma$, and assumption (4.5) holds with $\beta := \gamma$, immediately allowing one to conclude convergence in the sense of Theorem 2.6. In Section 5, we will show how this (sufficient, not necessary) condition can be experimentally verified, and that it holds for all cases considered.

4.5 Convergence to a statistical solution

In the previous section, we have shown that under external assumptions and up to a subsequence, the Monte Carlo scheme in Algorithm 4.1 converges to a correlation measure μ. In this section, we will prove a result akin to the Lax–Wendroff theorem, i.e. that said limit is a statistical solution to the incompressible Euler equations.

Theorem 4.7. *Let $\bar{\mu} \in \mathrm{Prob}(L^2(D; \mathbb{R}^d))$ with bounded support, $\mathrm{supp}(\bar{\mu}) \subset B_R(0) \subset L^2(D, \mathbb{R}^d)$ for some $R > 0$, with $\boldsymbol{u} \in L^2_{div}(D; \mathbb{R}^d)$ $\bar{\mu}$-almost surely. Let μ^h be given by (4.2) for $h > 0$, and assume that for some sequence $h_l \to 0$, the sequence $\{\mu^{h_l}\}_{l \in \mathbb{N}}$ converges strongly to $\mu \in L^1_t(\mathrm{Prob})$, in the sense of Theorem 2.6.III. Assume furthermore that there exists $\lambda > 0$ such that for all n, it holds that $\frac{\Delta t^n}{h} \leq \lambda$. Then μ is a statistical solution of the incompressible Euler equations.*

Proof. Let μ be the limit measure of μ^{h_l} as $l \to \infty$. μ is time-regular, as an immediate consequence of the uniform time-continuity of the approximations (Lemma 4.3), the convergence in Wasserstein norm (result (2.4) in Theorem 2.6), and Lemma 2.5. Thus, we need to verify that in the limit, properties 1 and 2 from Definition 2.7 are fulfilled.

Let us first verify the weak form of the incompressibility equation, (2.6). This is relatively straightforward. Fix $t \in [0, T)$. By Theorem 2.6.III, we have strong convergence for this observable. That

is,

$$\int_{L^2(D;\mathbb{R}^d)} \int_{D^2} (\boldsymbol{u}(x_1) \otimes \boldsymbol{u}(x_2)) : (\nabla\psi(x_1) \otimes \nabla\psi(x_2)) \, dx_1 dx_2 d\mu_t(\boldsymbol{u})$$

$$= \lim_{l\to\infty} \int_{L^2(D;\mathbb{R}^d)} \int_{D^2} (\boldsymbol{u}(x_1) \otimes \boldsymbol{u}(x_2)) : (\nabla\psi(x_1) \otimes \nabla\psi(x_2)) \, dx_1 dx_2 d\mu_t^{h_l}(\boldsymbol{u})$$

$$= \lim_{l\to\infty} \int_{L^2(D;\mathbb{R}^d)} \int_{D^2} \left(\mathcal{S}_t^{h_l}\overline{\boldsymbol{u}}(x_1) \otimes \mathcal{S}_t^{h_l}\overline{\boldsymbol{u}}(x_2)\right) : (\nabla\psi(x_1) \otimes \nabla\psi(x_2)) \, dx_1 dx_2 d\overline{\mu}^{h_l}(\overline{\boldsymbol{u}})$$

$$= \lim_{l\to\infty} \int_{L^2(D;\mathbb{R}^d)} \left(\int_D \mathcal{S}_t^{h_l}\overline{\boldsymbol{u}}(x) \cdot \nabla\psi(x) \, dx\right)^2 d\overline{\mu}^{h_l}(\overline{\boldsymbol{u}}) = 0.$$

To justify the last equality, let $\overline{\psi}$ be the cell averages of ψ. Recall that $\mathcal{S}_t^{h_l}\overline{\boldsymbol{u}}$ is $\overline{\mu}$-a.s. discretely divergence-free, and through Lemma 3.1, $\int_D \mathcal{S}_t^{h_l}\overline{\boldsymbol{u}}(x) \cdot \mathrm{grad}^h\overline{\psi}(x) \, dx = 0$. As ψ is smooth, some trivial Taylor analysis shows that $\|\mathrm{grad}^h\overline{\psi} - \nabla\psi\|_{L^\infty} \to 0$ uniformly, and thus the limit is zero.

Let us now show property 1. Let $\phi_1, \phi_2, \ldots, \phi_k \in C^\infty([0,T] \times D, \mathbb{R}^d)$ with $\nabla \cdot \phi_i = 0$ for all $i \in \{1, \ldots, k\}$; we must verify that

$$\int_0^T \int_{L^2(D;\mathbb{R}^d)} \int_{D^k} \left\{ [\boldsymbol{u}(t,x_1) \otimes \boldsymbol{u}(t,x_2) \otimes \cdots \otimes \boldsymbol{u}(t,x_k)] : \partial_t \Phi(t,\boldsymbol{x}) \right.$$

$$+ \sum_{\alpha=1}^k [\boldsymbol{u}(t,x_1) \otimes \cdots (\boldsymbol{u}(t,x_\alpha) \otimes \boldsymbol{u}(t,x_\alpha)) \otimes \cdots \otimes \boldsymbol{u}(t,x_k)] : \nabla_{x_i}\Phi(t,\boldsymbol{x}) \Big\} \, d\boldsymbol{x} \, d\mu_t(\boldsymbol{u}) \, dt$$

$$+ \int_{L^2(D;\mathbb{R}^d)} \int_{D^k} [\overline{\boldsymbol{u}}(x_1) \otimes \cdots \otimes \overline{\boldsymbol{u}}(x_k)] : \Phi(0,\boldsymbol{x}) \, d\boldsymbol{x} \, d\overline{\mu}(\overline{\boldsymbol{u}}) = 0,$$

where

$$\boldsymbol{x} := (x_1, x_2, \ldots, x_k) \in D^k, \qquad \Phi(t,\boldsymbol{x}) := \phi_1(t,x_1) \otimes \phi_2(t,x_2) \otimes \cdots \otimes \phi_k(t,x_k).$$

Fix $l \in \mathbb{N}$. For h_l, $\Pi_{h_l}^{div}$ induces in $\mathcal{G}_{h_l}^{d,div}$ the pushforward measure

$$\overline{\mu}^{h_l} := \Pi_{h_l}^{div} \# \overline{\mu}.$$

Let $\overline{\boldsymbol{u}}^{h_l} \in \mathrm{supp}(\overline{\mu}^{h_l})$ be a discretely divergence-free initial condition. For all $t \in [0,T]$, let

$$\boldsymbol{u}^{h_l}(t) := \mathcal{S}_t^{h_l}(\overline{\boldsymbol{u}}^{h_l});$$

and for all $i \in \{1, \ldots, k\}$, let $\phi_i^{h_l}(t) := \Pi_h^{div} \circ \phi_i(t,\cdot) \in \mathcal{G}_h^{d,div}$. Lemma 3.3.I guarantees that as $h_l \to 0$, $\|\phi^{h_l}(t) - \phi(t,\cdot)\|_{L^2(D;\mathbb{R}^d)}$ uniformly tends to zero. Let Φ^{h_l} be the spatially piecewise constant tensor function given, for all $\boldsymbol{j} = (j_1, \ldots, j_k)$, by

$$\Phi_{\boldsymbol{j}}^{h_l}(t,\boldsymbol{x}) := (\phi_1^{h_l})_{j_1}(t,x_1)(\phi_2^{h_l})_{j_2}(t,x_2)\cdots(\phi_k^{h_l})_{j_k}(t,x_k).$$

Denote for convenience $G(\boldsymbol{u},\boldsymbol{x},t) := \boldsymbol{u}(t,x_1) \otimes \boldsymbol{u}(t,x_2) \otimes \cdots \otimes \boldsymbol{u}(t,x_k)$; also $\overline{\mu}^{h_l}$-a.s. piecewise constant in space. Then

18

$$\int_0^T \int_{L^2(D;\mathbb{R}^d)} \int_{D^k} G(\boldsymbol{u}, \boldsymbol{x}, t) : \partial_t \Phi^{h_l} \, d\boldsymbol{x} \, d\mu_t^{h_l}(\boldsymbol{u}) \, dt$$

$$= \int_{L^2(D;\mathbb{R}^d)} \int_{D^k} \sum_{n=0}^{N(h_l)-1} \int_{t^n}^{t^{n+1}} G(\mathcal{S}_t^{h_l}(\boldsymbol{u}), \boldsymbol{x}, t) : \partial_t \Phi^{h_l} \, dt \, d\boldsymbol{x} \, d\bar{\mu}^{h_l}(\boldsymbol{u}). \tag{4.8}$$

Note that for all $x \in D$, $\boldsymbol{u}(\cdot, x)$ is $\bar{\mu}^{h_l}$-a.s. linear in $[t^n, t^{n+1}]$, so integrate by parts eq. (4.8) in time,

$$0 = \int_0^T \int_{L^2(D;\mathbb{R}^d)} \int_{D^k} G(\boldsymbol{u}, \boldsymbol{x}, t) : \partial_t \Phi^{h_l}(t, x) \, d\boldsymbol{x} \, d\mu_t^{h_l}(\boldsymbol{u}) \, dt$$

$$+ \int_{L^2(D;\mathbb{R}^d)} \int_{D^k} [\overline{\boldsymbol{u}}(x_1) \otimes \cdots \otimes \overline{\boldsymbol{u}}(x_k)] : \Phi^{h_l}(0, \boldsymbol{x}) \, d\boldsymbol{x} \, d\bar{\mu}^{h_l}(\overline{\boldsymbol{u}}) \tag{4.9}$$

$$+ \int_{L^2(D;\mathbb{R}^d)} \int_{D^k} \sum_{n=0}^{N(h_l)-1} \int_{t^n}^{t^{n+1}} \left[\partial_t G(\mathcal{S}_t^{h_l}(\boldsymbol{u}), \boldsymbol{x}, t) \right] : \Phi^{h_l}(t, \boldsymbol{x}) \, dt \, d\boldsymbol{x} \, d\bar{\mu}^{h_l}(\boldsymbol{u}).$$

Observe now that, as $\boldsymbol{u}^{h_l}(t, x) = \mathcal{S}_t^{h_l}\left(\overline{\boldsymbol{u}}^{h_l}(x)\right)$,

$$\partial_t G(\mathcal{S}_t^{h_l} \circ \boldsymbol{u}, \boldsymbol{x}, t) : \Phi^{h_l}(t, \boldsymbol{x}) = \sum_{\alpha=1}^k \left(\partial_t \boldsymbol{u}^{h_l}(t, x_\alpha) \cdot \phi_\alpha^{h_l}(t, x_\alpha) \right) \left(\prod_{\substack{\beta=1 \\ \beta \neq \alpha}}^k \boldsymbol{u}^{h_l}(t, x_\beta) \cdot \phi_\beta^{h_l}(t, x_\beta) \right). \tag{4.10}$$

For $t \in (t^n, t^{n+1})$ for any n, it holds $\mu_t^{h_l}$-a.s. that:

$$\partial_t \boldsymbol{u}^{h_l}(t) + \boldsymbol{C}^{h_l}(\boldsymbol{u}^{h_l;n}, \widetilde{\boldsymbol{u}}^{h_l;n+\frac{1}{2}}) - \boldsymbol{D}^{h_l}(\widetilde{\boldsymbol{u}}^{h_l;n+\frac{1}{2}}) - \text{grad}^{h_l} \psi^{h_l;n} = 0,$$

with all terms and operators as defined in Section 3. The integral of eq. (4.10) (as in (4.9)) can be rewritten with some reordering as

$$\int_{L^2(D;\mathbb{R}^d)} \int_{D^k} \sum_{n=0}^{N(h_l)-1} \int_{t^n}^{t^{n+1}} \left[\partial_t G(\mathcal{S}_t^{h_l}(\boldsymbol{u}), \boldsymbol{x}, t) \right] : \Phi^{h_l}(t, \boldsymbol{x}) \, dt \, d\boldsymbol{x} \, d\bar{\mu}^{h_l}(\boldsymbol{u})$$

$$= \sum_{\alpha=1}^k \int_{L^2(D;\mathbb{R}^d)} \sum_{n=0}^{N(h)-1} \int_{t^n}^{t^{n+1}} \left[\sum_{\boldsymbol{i} \in I} h_l^d \left(\boldsymbol{D}^{h_l}(\widetilde{\boldsymbol{u}}^{h_l;n+\frac{1}{2}})_{\boldsymbol{i}} + \text{grad}^{h_l} \psi_{\boldsymbol{i}}^{h_l;n} - \boldsymbol{C}^{h_l}(\boldsymbol{u}^{h_l;n}, \widetilde{\boldsymbol{u}}^{h_l;n+\frac{1}{2}})_{\boldsymbol{i}} \right) \cdot (\phi_\alpha^{h_l})_{\boldsymbol{i}}(t) \right]$$

$$\prod_{\substack{\beta=1 \\ \beta \neq \alpha}}^k \left[\sum_{\boldsymbol{i} \in I} h_l{}^d \boldsymbol{u}_{\boldsymbol{i}}^{h_l}(t) \cdot (\phi_\beta^{h_l})_{\boldsymbol{i}}(t) \right] \, dt \, d\mu^{h_l}(\boldsymbol{u}).$$

Let us now simplify the expression above. Due to the L^2 bound of the scheme, and the convergence in L^∞ of ϕ^{h_l} to ϕ (Lemma 3.3.III), it is immediate that for all $\beta \in \{1, \ldots, d\}$, and for all $t \in [0, T)$,

uniformly,

$$\sum_{\boldsymbol{i}\in I} h_l{}^d \boldsymbol{u}_{\boldsymbol{i}}^{h_l}(t)\cdot(\phi_\beta^{h_l})_{\boldsymbol{i}}(t) - \int_D \boldsymbol{u}^{h_l}(t,x)\cdot\phi_\beta(t,x)\,dx \stackrel{l\to\infty}{\longrightarrow} 0.$$

Lemma 3.2.V guarantees that $\bar\mu^{h_l}$-a.s., and for any $1\le\alpha\le k$,

$$\lim_{l\to\infty}\sum_{n=0}^{N(h)-1}\int_{t^n}^{t^{n+1}}\sum_{\boldsymbol{i}\in I} h_l{}^d \boldsymbol{D}^{h_l}(\widetilde{\boldsymbol{u}}^{h_l;n+\frac12})_{\boldsymbol{i}}\cdot(\phi_\alpha^{h_l})_{\boldsymbol{i}}(t)=0,$$

and this convergence is uniform. A direct application of Cauchy-Schwarz's inequality, together with the $\bar\mu$-a.s. L^2-boundedness of $\boldsymbol{u}$ and L^∞ boundedness of ϕ_i for all i (cf. Lemma 3.3.III), show that $\bar\mu$-a.s.,

$$\lim_{l\to\infty}\sum_{n=0}^{N(h)-1}\int_{t^n}^{t^{n+1}}\sum_{\alpha=1}^{k}\left[\sum_{\boldsymbol{i}\in I} h_l^d \boldsymbol{D}^{h_l}(\widetilde{\boldsymbol{u}}^{h_l;n+\frac12})_{\boldsymbol{i}}\cdot(\phi_\alpha^{h_l})_{\boldsymbol{i}}(t)\right]\prod_{\substack{\beta=1\\\beta\ne\alpha}}^{k}\left[\sum_{\boldsymbol{i}\in I} h_l^d \boldsymbol{u}_{\boldsymbol{i}}^{h_l}(t)\cdot(\phi_\beta^{h_l})_{\boldsymbol{i}}(t)\right]\,dt\,d\mu^{h_l}(\boldsymbol{u})=0.$$

Furthermore, as $\phi_i^{h_l}$ is $\bar\mu^{h_l}$-a.s. discretely divergence-free, $\bar\mu$-a.s., cf. Lemma 3.1, clearly

$$\sum_{\boldsymbol{i}\in I}\operatorname{grad}^{h_l}\psi_{\boldsymbol{i}}^{h_l;n}\cdot(\phi_\alpha^{h_l})_{\boldsymbol{i}}(t)=0.$$

Recall that $\boldsymbol{C}$ is defined as a difference of fluxes $\boldsymbol{F}^m$, which can be easily seen to be consistent, in the sense that $\boldsymbol{F}^m(\boldsymbol{u},\boldsymbol{u},\boldsymbol{u},\boldsymbol{u})=u_m\boldsymbol{u}$, and Lipschitz-continuous (under an assumption of L^2-boundedness of $\boldsymbol{u}$, cf. Lemma 3.2.II). A cumbersome but straightforward argument, cf. Parés-Pulido (2021), pp. 74-75, leveraging the properties listed in Lemmas 3.2 and 3.3, shows the following: for $t\in[t^n,t^{n+1})$,

$$\lim_{l\to\infty} h_l^d\sum_{\boldsymbol{i}\in I}-\boldsymbol{C}^{h_l}(\boldsymbol{u}^{h_l;n},\widetilde{\boldsymbol{u}}^{h_l;n+\frac12})_{\boldsymbol{i}}\cdot(\phi_\alpha^{h_l})_{\boldsymbol{i}}(t)$$

$$=\lim_{l\to\infty}\int_D\sum_{m=1}^{d}(u_m)^{h_l;n}(x)\boldsymbol{u}^{h_l;n}(x)\cdot\partial_{x_m}(\phi_\alpha)(t,x)\,dx$$

$$=\lim_{l\to\infty}\int_D\left[\boldsymbol{u}^{h_l;n}\otimes\boldsymbol{u}^{h_l;n}(x)\right]:\nabla(\phi_\alpha)(t,x)\,dx$$

Thus, substituting into eq. (4.9) and taking the limit as $l\to\infty$, we find

$$
0 = \lim_{l \to \infty} \left\{ \int_{L^2(D;\mathbb{R}^d)} \int_0^T \int_{D^k} [\boldsymbol{u}(t,x_1) \otimes \boldsymbol{u}(t,x_2) \otimes \cdots \otimes \boldsymbol{u}(t,x_k)] : \partial_t \Phi^{h_l} \; d\boldsymbol{x} \, dt \, d\mu^{h_l}(\boldsymbol{u}) \right.
$$

$$
+ \int_{L^2(D;\mathbb{R}^d)} \int_{D^k} [\overline{\boldsymbol{u}}(x_1) \otimes \cdots \otimes \overline{\boldsymbol{u}}(x_k)] : \Phi^{h_l}(0,\boldsymbol{x}) \; d\boldsymbol{x} \, d\bar{\mu}^{h_l}(\overline{\boldsymbol{u}})
$$

$$
+ \int_{L^2(D;\mathbb{R}^d)} \int_0^T \int_{D^k} \sum_{\alpha=1}^k [\boldsymbol{u}(t,x_1) \otimes \cdots \otimes (\boldsymbol{u}(t^n,x_\alpha) \otimes \boldsymbol{u}(t^n,x_\alpha)) \otimes \cdots \otimes \boldsymbol{u}(t,x_k)]
$$

$$
\left. : \nabla_{x_\alpha} \Phi(t,\boldsymbol{x}) \, d\boldsymbol{x} \, dt \, d\mu^{h_l}(\boldsymbol{u}) \right\}
$$

Note that the term $(\boldsymbol{u}(t^n,x_\alpha) \otimes \boldsymbol{u}(t^n,x_\alpha))$ remains not parameterized with respect to t. However, it is not difficult to show, Parés-Pulido (2021), Corollary A.19, that the integral of $(\boldsymbol{u}(t^n,x_\alpha) \otimes \boldsymbol{u}(t^n,x_\alpha)) - (\boldsymbol{u}(t,x_\alpha) \otimes \boldsymbol{u}(t,x_\alpha))$ vanishes in the limit. Hence, additionally replacing ϕ^{h_l} and Φ^{h_l} by their continuous counterparts, again through the L^2-boundedness of $\boldsymbol{u}$ and the L^∞-convergence of ϕ^{h_l} to ϕ (Lemma 3.3.III) we conclude that

$$
0 = \lim_{l \to \infty} \left\{ \int_{L^2(D;\mathbb{R}^d)} \int_0^T \int_{D^k} [\boldsymbol{u}(t,x_1) \otimes \boldsymbol{u}(t,x_2) \otimes \cdots \otimes \boldsymbol{u}(t,x_k)] : \partial_t \Phi \; d\boldsymbol{x} \, dt \, d\mu^{h_l}(\boldsymbol{u}) \right.
$$

$$
+ \int_{L^2(D;\mathbb{R}^d)} \int_{D^k} [\overline{\boldsymbol{u}}(x_1) \otimes \cdots \otimes \overline{\boldsymbol{u}}(x_k)] : \Phi(0,\boldsymbol{x}) \; d\boldsymbol{x} \, d\bar{\mu}^{h_l}(\overline{\boldsymbol{u}})
$$

$$
+ \int_{L^2(D;\mathbb{R}^d)} \int_0^T \int_{D^k} \sum_{\alpha=1}^k [\boldsymbol{u}(t,x_1) \otimes \cdots \otimes (\boldsymbol{u}(t,x_\alpha) \otimes \boldsymbol{u}(t,x_\alpha)) \otimes \cdots \otimes \boldsymbol{u}(t,x_k)]
$$

$$
\left. : \nabla_{x_\alpha} \Phi(t,\boldsymbol{x}) \, d\boldsymbol{x} \, dt \, d\mu^{h_l}(\boldsymbol{u}) \right\}
$$

$$
= \int_{L^2(D;\mathbb{R}^d)} \int_0^T \int_{D^k} [\boldsymbol{u}(t,x_1) \otimes \boldsymbol{u}(t,x_2) \otimes \cdots \otimes \boldsymbol{u}(t,x_k)] : \partial_t \Phi \; d\boldsymbol{x} \, dt \, d\mu(\boldsymbol{u})
$$

$$
+ \int_{L^2(D;\mathbb{R}^d)} \int_{D^k} [\overline{\boldsymbol{u}}(x_1) \otimes \cdots \otimes \overline{\boldsymbol{u}}(x_k)] : \Phi(0,\boldsymbol{x}) \; d\boldsymbol{x} \, d\bar{\mu}(\overline{\boldsymbol{u}})
$$

$$
+ \int_{L^2(D;\mathbb{R}^d)} \int_0^T \int_{D^k} \sum_{\alpha=1}^k [\boldsymbol{u}(t,x_1) \otimes \cdots \otimes (\boldsymbol{u}(t,x_\alpha) \otimes \boldsymbol{u}(t,x_\alpha)) \otimes \cdots \otimes \boldsymbol{u}(t,x_k)]
$$

$$
: \nabla_{x_\alpha} \Phi(t,\boldsymbol{x}) \, d\boldsymbol{x} \, dt \, d\mu(\boldsymbol{u}).
$$

In the last step, we have used the assumption of convergence in the sense of Theorem 2.6.III. That is: the limit measure verifies the momentum equation (2.5), and is indeed, a statistical solution of the incompressible Euler equations.

$\square$

Remark 4.8. *In fact, under the conditions of Theorem 4.7, the limit μ_t can be seen to be a **dissipative statistical solution** in the sense of Def. 2.8. The fundamental observation is that energy is an admissible observable in the sense of Theorem 2.6.III; the proof for the convex splitting is tedious but straightforward. Cf. Remark 4.6 in Lanthaler et al. (2021). In particular, then Theorems 2.9 and 2.10 for well-posedness hold.*

5   Numerical examples

The Monte Carlo algorithm 4.1 is eminently practical; we present here some novel numerical examples, for well-known test cases, computed with the implementation of the scheme in Leonardi (2017a).

5.1   Setting and notation

Regarding the numerical parameters for scheme (3.1)-(3.2), we consider $\theta = 1$, a coefficient for numerical viscosity $\epsilon = 0.1$, and a time-step that satisfies a CFL-type condition for the underlying advection problem with CFL number $\lambda = 0.5$.

Let $N, M \in \mathbb{N}$, $T \in \mathbb{R}$. We will denote an **ensemble** of M simulations at resolution $N \times N$ up to time T by

$$U^{N,M,T} := \{U^{N,m,T}\}_{m=1}^M,$$

where each $U^{N,m,T}$, dubbed **sample**, is a separate realization of a Cauchy problem on an $N \times N$ grid, up to time T, as described in Algorithm 4.1.

Remark 5.1. *Fixing t, an ensemble $U^{N,M,t}$ can be trivially identified with a probability distribution $\mu_t \in \mathrm{Prob}(L^p(D; \mathbb{R}^d))$, which we term its **empirical measure**:*

$$\mu_t^{N,M} = \frac{1}{M} \sum_{m=1}^M \delta_{U^{N,m,t}}. \tag{5.1}$$

A priori, the number M of samples in Algorithm 4.1 and the spatial resolution N of the finite volume scheme are unrelated. However, to ensure convergence as the mesh is refined, we make the choice of equating $M = N$. Even in two dimensions, the cost of higher-resolution simulations makes it prohibitive to scale M like N^2 (as a naive Monte Carlo approximation would have); we remark however that the convergence proven in Theorems 4.4 and 4.7 is without a rate. This choice is frequent in the literature, see e.g. Fjordholm et al. (2018), Fjordholm et al. (2020), Lanthaler et al. (2021)...

In this section we will often refer, for a time t, to the **sample mean** and **variance operators**, defined as those of the empirical measure.

For the discretization of the structure function, we will follow the choices of Lye (2020) and take

$$
\int_D \fint_{B_r(x)} \|\boldsymbol{u}(y) - \boldsymbol{u}(x)\|^p \, dy \, dx
$$

$$
\approx \frac{h^2}{l^2} \sum_{i=1}^{N} \sum_{j=1}^{N} \Bigg[\sum_{k=-l+1}^{l} \sum_{n=-l+1}^{l} \left(\|U_{i+k,j+n} - U_{i,j}\|^p \right)
$$

$$
+ \frac{1}{2} \sum_{k=-l+1}^{l} \left(\|U_{i+k,j-l} - U_{i,j}\|^p + \|U_{i+k,j+l} - U_{i,j}\|^p \right)
$$

$$
+ \frac{1}{2} \sum_{n=-l+1}^{l} \left(\|U_{i-l,j+n} - U_{i,j}\|^p + \|U_{i+l,j+n} - U_{i,j}\|^p \right)
$$

$$
+ \frac{1}{4} \sum_{\alpha,\beta=0}^{1} \|U_{i+(-1)^\alpha l, j+(-1)^\beta l} - U_{i,j}\|^p \Bigg].
$$

For reasons of computational efficiency, we will present structure functions at fixed times, i.e. for a given $t \in [0, T)$ we compute

$$
S_{r,t}^p(\boldsymbol{\nu}) := \left(\int_{L_x^p} \int_D \fint_{B_r(x)} \|\boldsymbol{u}(y) - \boldsymbol{u}(x)\|^p \, dy \, dx \, d\mu_t(u) \right)^{\frac{1}{p}}.
$$

As will be shown in the sequel, we observe uniform bounds for all time points considered for all numerical cases. This is strong evidence for uniform boundedness for the time-integrated version, and thus for convergence (up to a subsequence) of the scheme; compare to Remark 4.6.

5.2 Double shear layers

Here we present two tests in a well-known family, the two-dimensional double *shear layer*.

We dub *smooth shear layer* the following initial datum: fix $\rho > 0$, and consider the initial condition for $(x, y) \in \mathbb{T}^2$:

$$
\tilde{u}_0(x, y) = \begin{cases} \tanh\left((y - 0.25)/\rho\right) & \text{if } y \leq 0.5, \\ \tanh\left((0.75 - y)/\rho\right) & \text{otherwise;} \end{cases} \qquad \tilde{v}_0(x, y) = 0.
$$

The *discontinuous shear layer* is the formal limit of the above when $\rho \to 0$; that is,

$$
\tilde{u}_0(x, y) = \begin{cases} 1 & \text{if } y \in (0.25, 0.75), \\ -1 & \text{otherwise;} \end{cases} \qquad \tilde{v}_0(x, y) = 0.
$$

The *smooth* initial datum satisfies the conditions for local existence of classical solutions of the incompressible Euler equations. Therefore, at least for a short time horizon, one can expect the existence of a unique strong solution; and thus, due to weak-strong uniqueness, see Brenier et al. (2011); also cf.

Theorem 2.10, as long as the classical solution is defined, there exists a unique measure-valued solution, and that is the atomic measure corresponding to the classical solution.

Conversely, the ***discontinuous*** initial datum has vorticity which is a measure without distinguished sign, so it falls outside of Delort's class; in fact it is explicitly known, Székelyhidi (2011), to belong to the class of "wild initial data", i.e. there are infinitely many (admissible) weak solutions to this problem.

Fix now $0 < \gamma \in \mathbb{R}$, $K \in \mathbb{N}$ even, and consider a random perturbation function

$$f_\gamma : \Omega \times \mathbb{T}^2 \to \mathbb{T}^2$$

$$f_\gamma(\omega; x, y) = \left(x, y + \gamma \sum_{k=0}^{K/2} Y_{2k}(\omega) \sin(2\pi(k+1)(x + Y_{2k+1}(\omega))) \right), \tag{5.2}$$

with $Y_j \sim \mathcal{U}[-1, 1]$ i.i.d. $\forall j$. Finally, set initial velocities

$$(u_0, v_0)(\omega, \cdot) = (\tilde{u}_0, \tilde{v}_0) \circ f_\gamma(\omega; \cdot);$$

we recall that discrete divergence is projected out (with operator Π_h^{div}) before simulation starts. See Fig. 1 for an example of the effect of the perturbation on the initial condition.

Let us first remark that, for individual realizations of the Cauchy problem, the two variants of the initial datum exhibit drastically different evolutions. In Fig. 2 we present, at different points in time t, the Cauchy rates $\|\boldsymbol{u}^h(t) - \boldsymbol{u}^{\frac{h}{2}}(t)\|_{L^2}$ for discretizations of the same realization of the initial datum. Clearly as the mesh is refined, the smooth shear layer, at all times, appears to form a Cauchy sequence in L^2; the same is only true for the discontinuous version at $t = 0$; for all later times, the Cauchy rate appears to flatten rapidly.

In Fig. 3 we display the structure functions obtained for both cases at times $t \in \{0, 0.4\}$. The uniform boundedness appears obvious; in fact the initial data for the discontinuous shear layer gains regularity as the simulation evolves, due to the action of the numerical diffusion operator $\boldsymbol{D}$ – which, recall Lemma 3.2.V, vanishes in the limit. Hence, through Theorems 4.4-4.7, one can expect convergence (up to a subsequence) of Algorithm 4.1.

In fact, we find direct numerical evidence of this convergence for the sequence of resolutions considered. Let $\boldsymbol{\nu}_t^{N,N}$ the correlation measure associated, in the sense of Theorem 2.3, with the empirical measure $\mu_t^{N,N}$ in eq. (5.1). In Fig. 4 we display the Cauchy rates for an approximation to the Wasserstein distances for the k-point marginals $\boldsymbol{\nu}_t^{k;N,N}$, i.e., we plot

$$W_1\left(\boldsymbol{\nu}^{k;N,N}, \boldsymbol{\nu}^{k;2N,2N}\right),$$

as a function of N, for $k \in \{1, 2, 3\}$. The results strongly suggest convergence (albeit noisy) of the marginal probability measures. In fact, as Theorem 2.6 indicates, observables such as mean and variance of the empirical measure, considered as functions in L^2, converge strongly; cf. Fig. 5.

We believe this test case paints a convincing picture of the advantage of the framework of statistical solutions: weak, deterministic solutions appear an unsuitable framework for numerics (Fig. 2), at least for cases where no unique solution exists. Conversely, we obtain solid experimental evidence that assumption (4.5), necessary for convergence of statistical solutions, holds for both cases (Fig. 3). Indeed, as predicted by Theorem 2.6 we observe strong convergence for observables such as mean and variance. Furthermore,
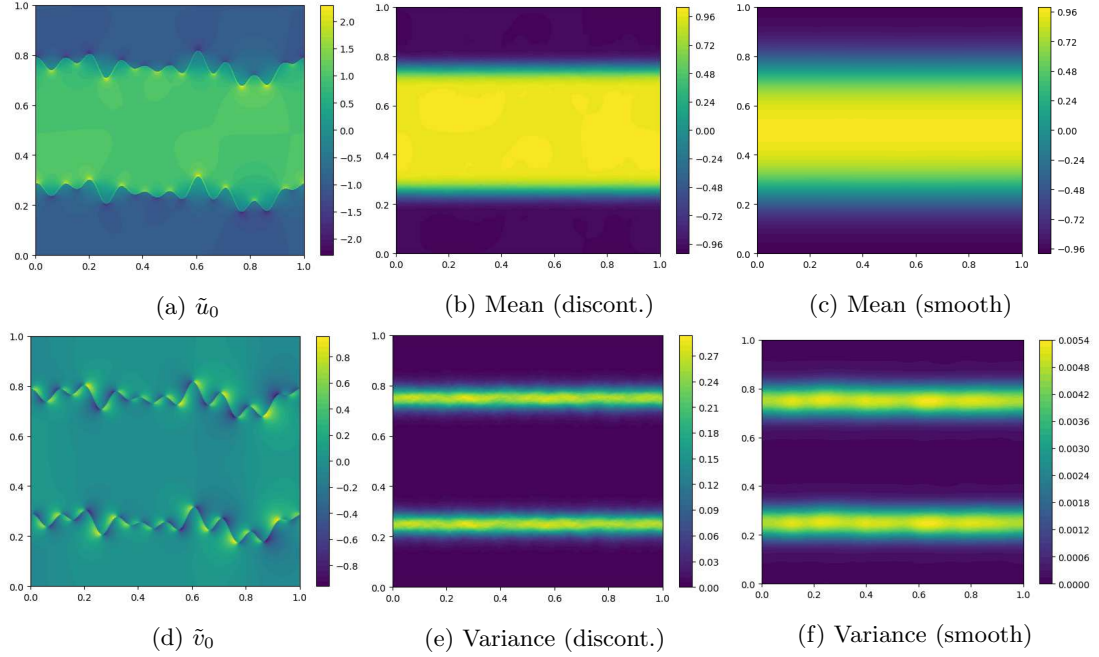
Figure 1: Left: one realization of the random initial condition for discontinuous shear layer. Center: mean (top) and variance (bottom) for $\tilde{u}_0$, discontinuous shear layer. Right: mean and variance for $\tilde{u}_0$, smooth shear layer.
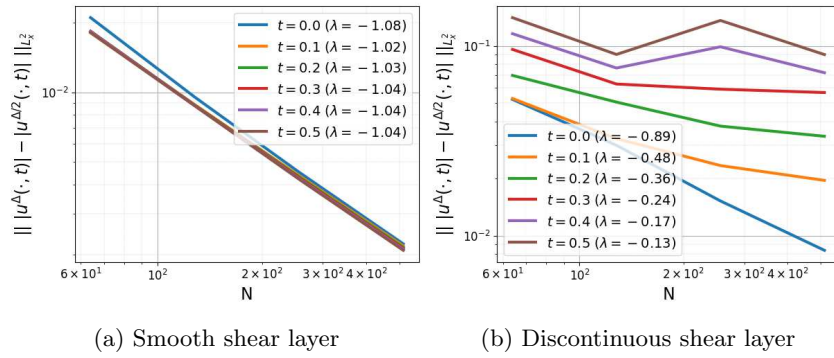

Figure 2: Cauchy rates for individual samples as time evolves, for smooth (left) and discontinuous (right) shear layer. λ is the least square fit for the slope.
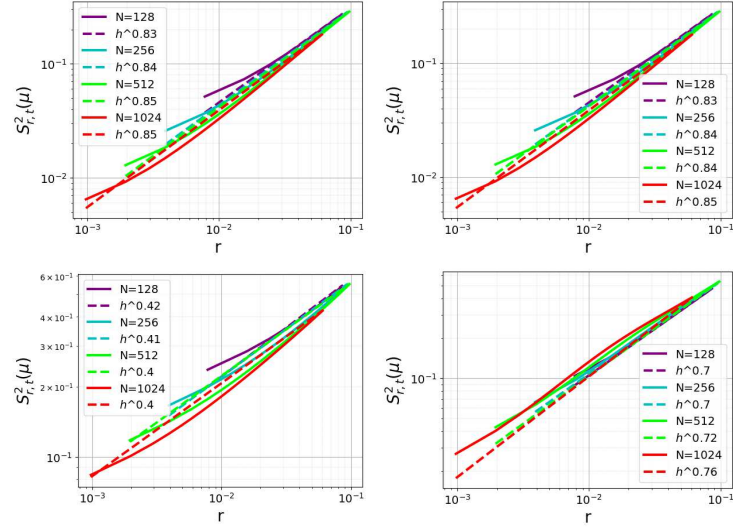
Figure 3: Structure functions for velocity vector, $p = 2$, for smooth (top) and discontinuous shear layer (bottom). Left, $t = 0$; right, $t = 0.4$.

(a) $k = 1$ (b) $k = 2$ (c) $k = 3$

(d) $k = 1$ (e) $k = 2$ (f) $k = 3$
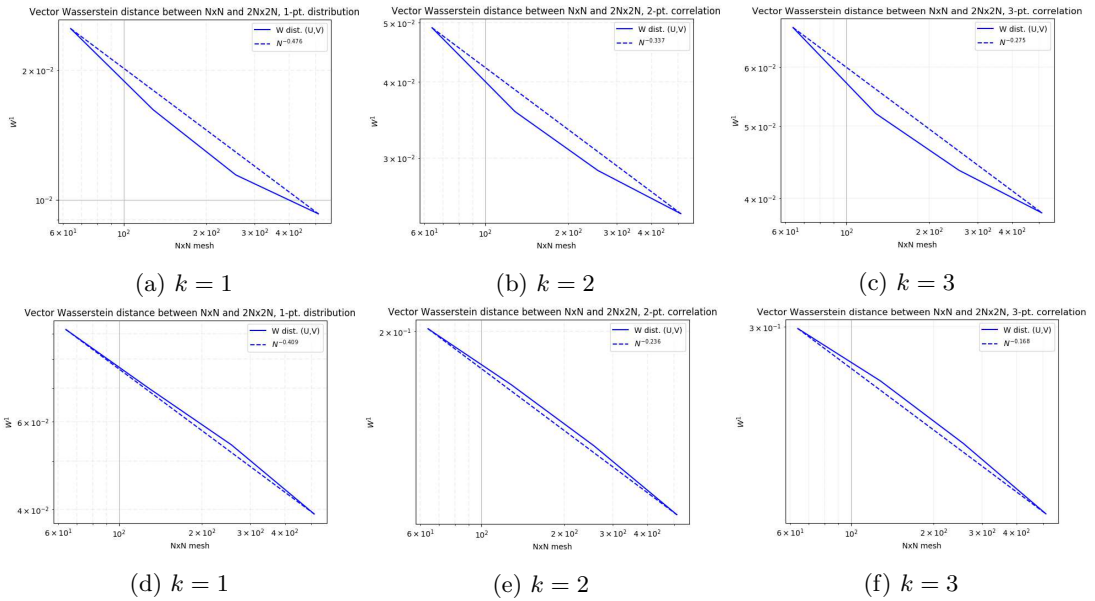
Figure 4: Cauchy rates for Wasserstein distances for the velocity vector field, (left to right) 1-, 2- and 3-point marginals. Smooth (top) and discontinuous (bottom) shear layer; $t = 0.4$.

26

(a) Smooth shear layer   (b) Discontinuous shear layer
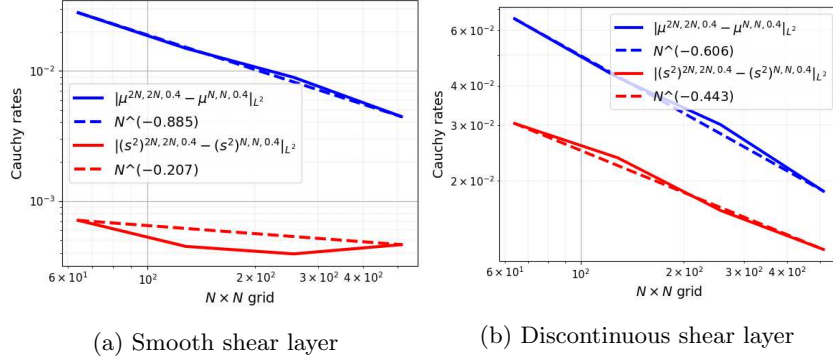
Figure 5: Cauchy rates for mean and variance for the smooth (left) and discontinuous (right) shear layer.

we find evidence that the marginals converge, even for $k > 1$; i.e. we do not only obtain convergence in the sense of measure-valued solutions, but properly for statistical solutions.

5.2.1 Convergence to a non-trivial statistical solution

In this section, we briefly present a result we find enlightening about the shear layer numerical experiment. As mentioned before, there is a fundamental difference in well-posedness for the smooth and discontinuous shear layer. However, in the numerical experiments above, we have found fairly analogous results for both, up to slightly faster rates of convergence for the smooth version. With the following example, we aim to show a key difference between the empirical measure obtained for both cases.

For this, recall (5.2): we introduced a perturbation f_γ, with a "small" parameter γ. An interesting question is: what changes if one lets $\gamma \to 0$? Does one recover the unperturbed initial datum $(\tilde{u}_0, \tilde{v}_0)$, itself a steady state, as a solution to the problem? In other words: fix a high enough resolution N (we take $N = 1024$ here), and for $\gamma > 0$, denote μ_γ the empirical measure $\mu_t^{N,\tilde{N}}$ obtained with initial data distributed as $(\tilde{u}_0, \tilde{v}_0) \circ f_\gamma$. Consider the stationary solution $\bar{\boldsymbol{u}}(t) := (\tilde{u}_0, \tilde{v}_0)$ for all $t \geq 0$. Is it true that

$$\lim_{\gamma \to 0} W_1(\mu_{\gamma,t}, \delta_{\bar{\boldsymbol{u}}}) = 0?$$

The answer can be found in Fig. 6. If one takes a very small value of γ as a "reference solution", one can see that both examples appear to converge to the reference solution. However, the distance to $\delta_{\bar{\boldsymbol{u}}}$ only appears to tend to zero for the smooth shear layer. This corresponds to the theoretical intuition: in that case, there exists a unique classical solution, and the only statistical solution is its atomic measure, due to weak-strong uniqueness. Conversely, infinitely many weak solutions exist for the discontinuous shear layer, and thus even as $\gamma \to 0$, we do not recover an atomic measure, but a non-trivial statistical solution.

5.3 Fractional Brownian motions

A **fractional Brownian motion**, Kolmogorov (1940), Mandelbrot & Van Ness (1968), with **Hurst index** $H \in [0, 1)$ is a random noise field $X_H : \Omega \times D \to \mathbb{R}$, that takes normally-distributed values with
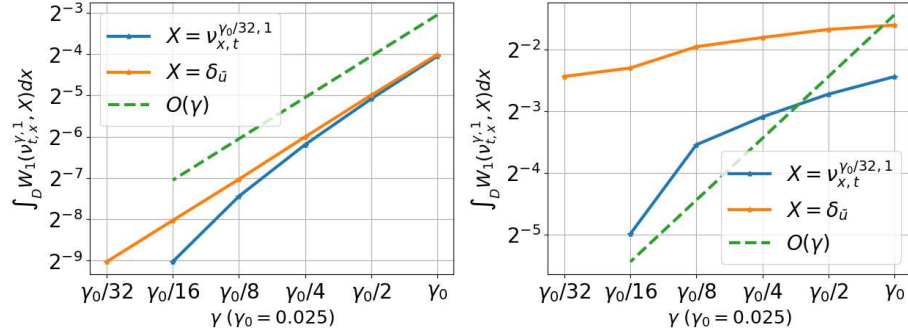
Figure 6: Wasserstein distances with respect to a very small perturbation (blue) and the unperturbed initial datum (orange) as the perturbation magnitude reduces. Smooth (left) and discontinuous (right) shear layer; 1-point marginals at time $t = 0.4$.
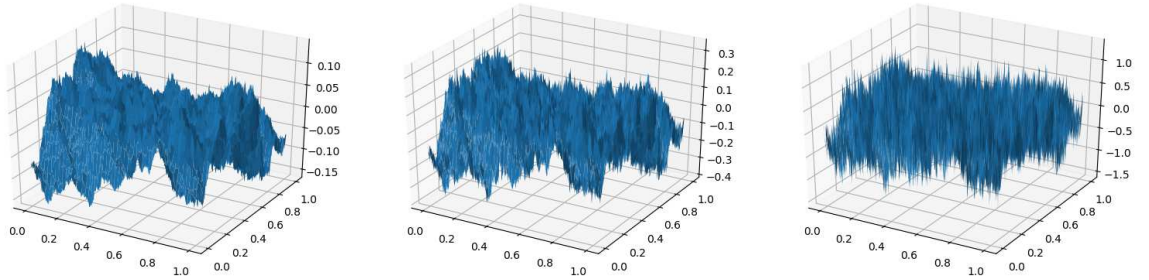

Figure 7: Three realizations of horizontal velocity for initial data in a fractional Brownian motion (left to right: $H = 0.75$, $H = 0.5$, $H = 0.15$) after discretely divergence-free projection.

mean zero at each point, and has covariance

$$\text{Cov}[X_H(x), X_H(y)] = \mathbb{E}\left[X_H(x)X_H(y)\right] = \frac{1}{2}(\|x - y\|^{2H} - \|x\|^{2H} - \|y\|^{2H}).$$

The case $H = 0.5$ corresponds to a Brownian motion, often referred to as having "independent increments"; this is not the case for $H \neq 0.5$. A realization of a Brownian motion with Hurst index H is a.e. in $C^{0,\alpha}(D)$, with $\alpha \leq \max\{0, H - \epsilon\}$ for all $\epsilon > 0$, Prop. 6.4.2 in Leonardi (2018a). We display here that, even for low Hölder-regularity settings, assumption (4.5) holds. We generate realizations of fractional Brownian motions[1] with the midpoint displacement method, Lévy (1992), Lambert-Lacroix et al. (2007).

We present here results for $H \in \{0.75, 0.5, 0.15\}$; we include a realization of the initial data for each in Fig. 7.

We display in Fig. 8 the structure function, for $t \in \{0, 1\}$, for all three cases. We observe, again, an initial exponent roughly corresponding to H, and a regularization effect as time advances. In Fig. 9 we

---

[1]More accurately, Brownian bridges, due to the periodic boundary conditions.
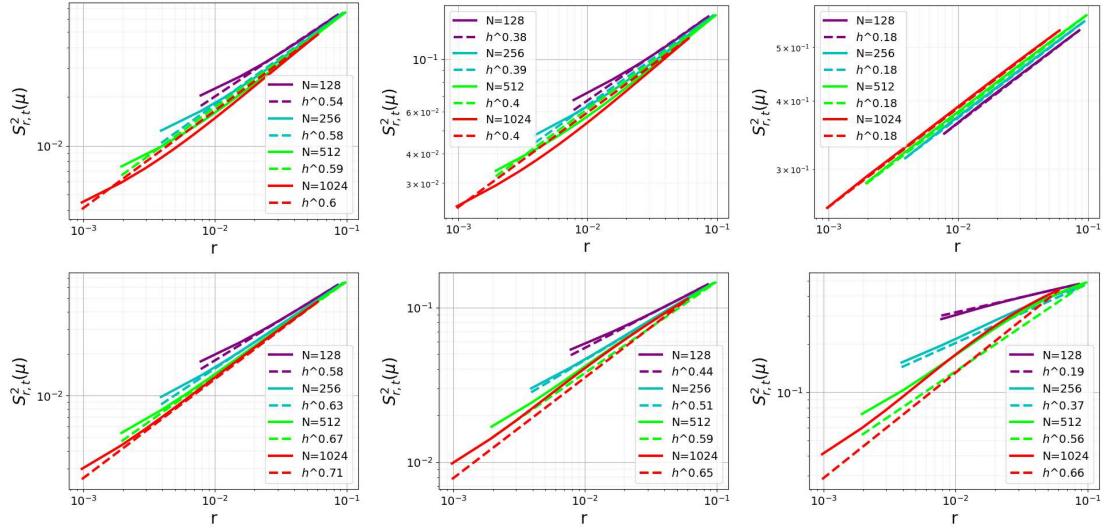
Figure 8: Structure functions for velocity vector, $p = 2$, for fractional Brownian motion with (left to right) $H \in \{0.75, 0.5, 0.15\}$, for $t = 0$ (top) and $t = 1$ (bottom).

include the evolution of the fitted slope with time, clearly illustrating this.

Again, a uniform boundedness from above is strongly suggested, even for initial data in very low regularity spaces. Unsurprisingly again, we observe clear strong convergence of observables (Fig. 10) and vanishing Cauchy rates in Wasserstein metric, for the first few marginals, as in the previous test (Fig. 11).

5.4 Stability

In this paper, we have discussed only the version of Algorithm 4.1 which uses the finite volume scheme (3.1)-(3.2) as an underlying method.
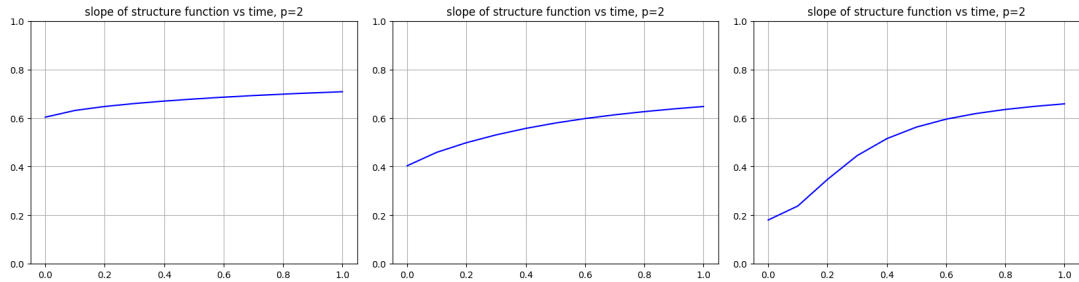
Figure 9: Time evolution of the best fit for the slope, as in Fig. 8, for the structure function with $p = 2$. Left to right, $H = 0.75$, $H = 0.5$, $H = 0.15$.
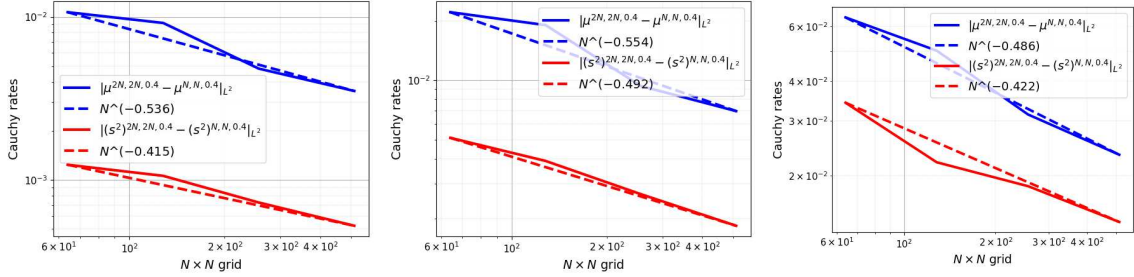
Figure 10: Cauchy rates for mean and variance for fractional Brownian motions; left to right, $H = 0.75$, $H = 0.5$, $H = 0.15$, at time $t = 1$.
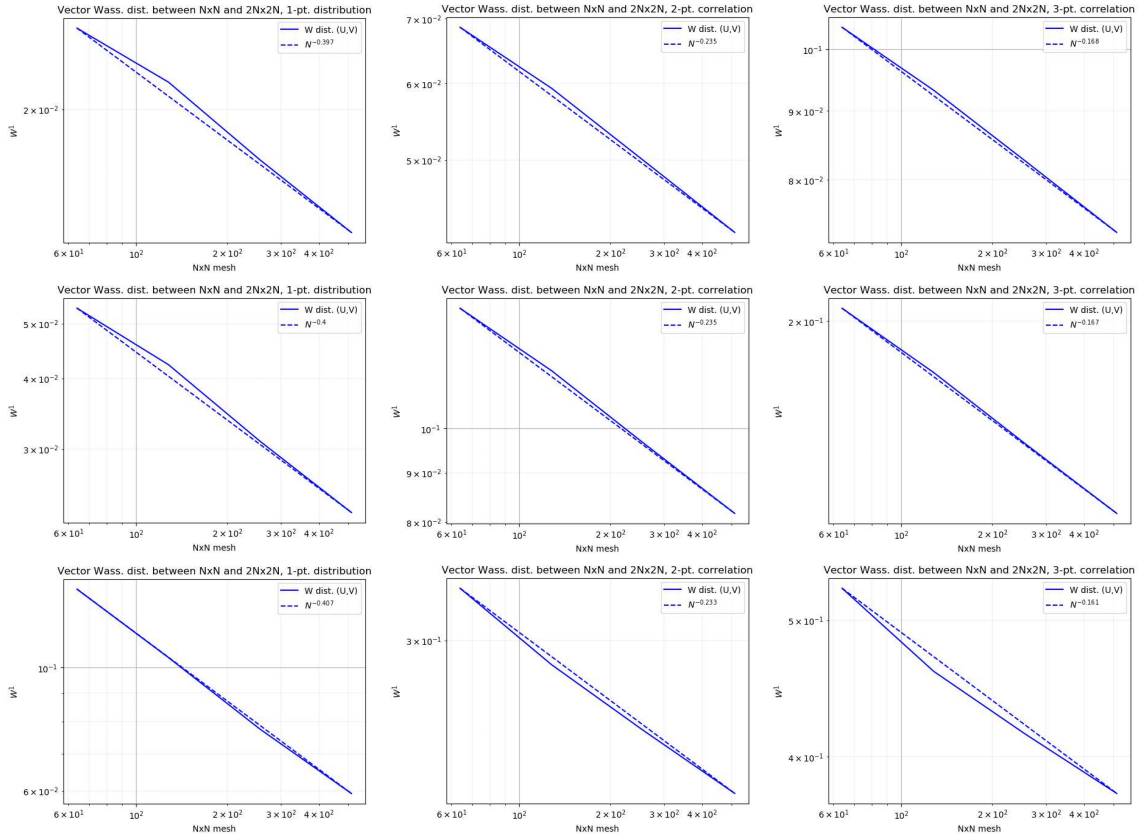

Figure 11: Cauchy rates for Wasserstein distances for the velocity vector field, (left to right) 1-, 2- and 3-point marginals at $t = 1$. Top to bottom, $H = 0.75$, $H = 0.5$, $H = 0.15$.

(a) 1-pt distributions

(b) 2-pt correlations
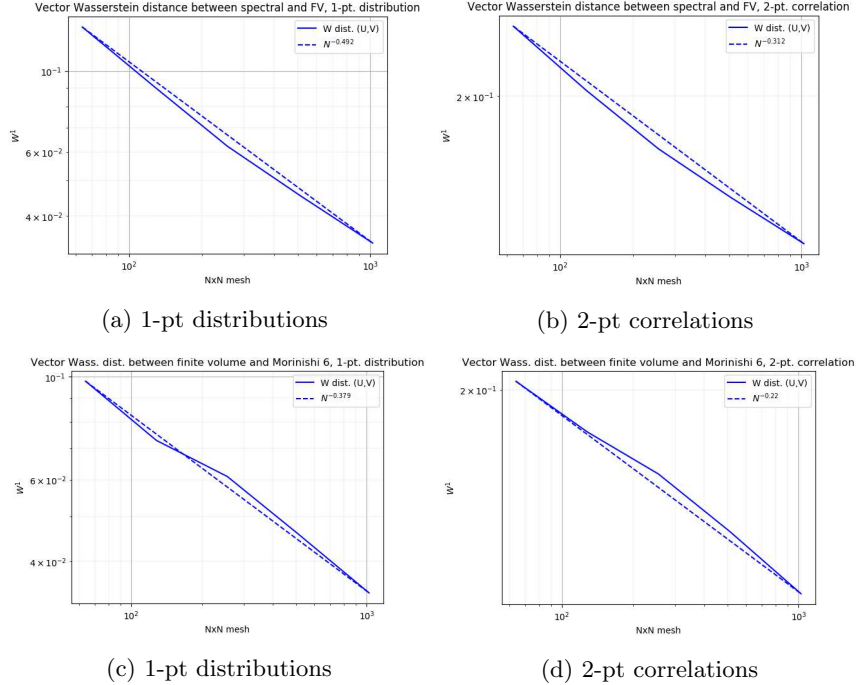

(c) 1-pt distributions

(d) 2-pt correlations

Figure 12: Wasserstein distance (left: one-point marginals; right: two-point marginals) between finite volume and hyperviscosity spectral solver Lanthaler et al. (2021), top; and between finite volume and 6th order Morinishi Morinishi et al. (1998), bottom. Distance is measured at the same resolution and number of samples for both solvers, 64×64 to 1024×1024.

We believe that Algorithm 4.1 is robust with respect to the choice of the underlying solver. To this effect, we have run identical simulations with the following numerical schemes: the hyperviscosity spectral scheme of Lanthaler et al. (2021), with the implementation in Leonardi (2017b); the high-order ENO finite difference scheme of Mishra et al. (2021), and the high-order finite difference central scheme of Morinishi et al. (1998). For all of them, we observe similar results, and in fact the Wasserstein distance between the marginals computed with different schemes appears to tend to zero as the resolution is increased. See Fig. 12 for some examples for the discontinuous shear layer; this is chosen for brevity as other examples display identical results.

Furthermore, we also remark that for the case of deterministic initial data, we have suggested an arbitrary perturbation. Numerical experiments suggest that the choice of perturbation is, as the magnitude goes to zero, of little practical consequence.

6   Conclusions and future work

In this work we have presented an algorithm for the efficient computation of statistical solutions, rigorously proven its convergence, and displayed its practical use.

As stated in Theorem 4.4, this convergence is only up to a subsequence, and conditioned to an external ***scaling assumption*** on the structure function. However, in section 5, we have shown some numerical experiments that give credibility to the claim that this assumption is relatively mild, and in two dimensions it holds for every numerical experiment considered.

Furthermore, we find that the results obtained are fully consistent with those found in the literature, e.g. Lanthaler et al. (2021) for spectral methods. This supports the idea that a Monte Carlo algorithm, presented here as 4.1, can be non-intrusively applied over any standard scheme in the literature.

In particular, the crucial novel result of this work is that a finite volume scheme can be used for this goal. To the knowledge of the author, the only analogous previously existing results are those of Lanthaler et al. (2021), for spectral schemes. These, although highly efficient, are suitable only for a very limited selection of problems, in simple domains with periodic boundary conditions. Although the results presented here are derived in the torus, this is a technical assumption for convenience; there is every reason to believe they hold analogously for other types of periodic boundary conditions. In fact, we remark that in Parés-Pulido (2021), Section 6.3, an example of a channel flow with no-flow boundary conditions is presented, where the scaling assumption holds as well.

Algorithm 4.1 presented here is based on a relatively coarse Monte Carlo integration. Techniques such as multi-level Monte Carlo methods, quasi Monte Carlo, etc. could be applied to accelerate the convergence and reduce the amount of high-resolution samples needed. Some attempts exist in the literature at applying these, e.g. Leonardi (2018a), Lye (2020), but their success has been limited. Analogously, in Parés-Pulido (2021) we study the possible application of high-order schemes, in space and time; we find that these do not appear to produce significant gains.

This strongly suggests that, if the rate of the convergence is to be improved, the bottleneck is in the Monte Carlo sampling. In fact, we have only presented two-dimensional numerical experiments here. The theory, as derived here, holds for higher dimensions as well; the limitation to two-dimensional problems is due to computational constraints. There is presently ongoing work, Rohner (2021), to develop an efficient, highly-parallelizable three-dimensional solver to carry out the corresponding experiments.

Nonetheless, we believe that this work extends the state of the art and provides consistent evidence that a Monte Carlo scheme can be combined with any well-known numerical method for the incompressible Euler equations to produce statistical solutions. Similar conclusions have been reached in e.g. Fjordholm et al. (2020) for systems of conservation laws (including the compressible Euler equations), furthering the credibility that statistical solutions, approximated through Monte Carlo integration, are a satisfactory technique for the solution of partial differential equations, both as a sound theoretical framework and as a practically tractable approach.

References

Beale, J. T., Kato, T. & Majda, A. (1984), 'Remarks on the breakdown of smooth solutions for the 3-D Euler equations', *Communications in Mathematical Physics* **94**(1), 61–66.

Bell, J. B., Colella, P. & Glaz, H. M. (1989), 'A second-order projection method for the incompressible Navier-Stokes equations', *Journal of Computational Physics* **85**(2), 257–283.

Brenier, Y., De Lellis, C. & Székelyhidi, L. (2011), 'Weak-strong uniqueness for measure-valued solutions', *Communications in Mathematical Physics* **305**, 351–361.

Buckmaster, T. & Vicol, V. (2019), 'Nonuniqueness of weak solutions to the Navier-Stokes equation', *Annals of Mathematics* **189**(1), 101–144.

De Lellis, C. & Székelyhidi, Jr, L. (2009), 'The Euler equations as a differential inclusion', *Annals of Mathematics* **170**(3), 1417–1436.

De Lellis, C. & Székelyhidi, Jr., L. (2013), 'Dissipative continuous Euler flows', *Inventiones mathematicae* **193**(2), 377–407.

Delort, J.-M. (1991), 'Existence de nappes de tourbillon en dimension deux', *J. Am. Math. Soc.* **4**(3), 553–586.

DiPerna, R. J. (1985), 'Measure-valued solutions to conservation laws', *Archive for Rational Mechanics and Analysis* **88**(3), 223–270.

DiPerna, R. J. & Majda, A. J. (1987), 'Oscillations and concentrations in weak solutions of the incompressible fluid equations', *Communications in Mathematical Physics* **108**(4), 667–689.

Epstein, E. S. (1969), 'Stochastic dynamic prediction', *Tellus* **21**(6), 739–759.

Fefferman, C. (2006), 'Existence and smoothness of the Navier-Stokes equation', *The Millennium Prize Problems* .

Feireisl, E., Lukáčová-Medviďová, M. & Mizerová, H. (2020), '$\mathcal{K}$-convergence as a new tool in numerical analysis', *IMA Journal of Numerical Analysis* **40**(4), 2227–2255.

Fjordholm, U. S., Käppeli, R., Mishra, S. & Tadmor, E. (2017), 'Construction of approximate entropy measure-valued solutions for hyperbolic systems of conservation laws', *Foundations of Computational Mathematics* **17**(3), 763–827.

Fjordholm, U. S., Lanthaler, S. & Mishra, S. (2017), 'Statistical solutions of hyperbolic conservation laws: Foundations', *Archive for Rational Mechanics and Analysis* **226**(2), 809–849.

Fjordholm, U. S., Lye, K. & Mishra, S. (2018), 'Numerical approximation of statistical solutions of scalar conservation laws', *SIAM Journal on Numerical Analysis* **56**(5), 2989–3009.

Fjordholm, U. S., Lye, K., Mishra, S. & Weber, F. (2020), 'Statistical solutions of hyperbolic systems of conservation laws: Numerical approximation', *Mathematical Models and Methods in Applied Sciences* **30**(03), 539–609.

Fjordholm, U. S., Mishra, S. & Tadmor, E. (2016), 'On the computation of measure-valued solutions', *Acta Numerica* **25**.

Foias, C. (1973), 'Statistical study of Navier-Stokes equations, II', *Rendiconti del Seminario Matematico della Universita di Padova* **49**, 9–123.

Foias, C., Rosa, R. & Temam, R. (2013), Properties of time-dependent statistical solutions of the three-dimensional Navier-Stokes equations, *in* 'Annales de l'Institut Fourier', Vol. 63(6), pp. 2515–2573.

Frisch, U. & Kolmogorov (1995), *Turbulence: the legacy of A. N. Kolmogorov*, Cambridge University Press.

Kolmogorov, A. N. (1940), 'Wienersche Spiralen und einige andere interessante Kurven in Hilbertschen Raum', *Acad. Sci. URSS (NS)* **26**, 115–118.

Ladyzhenskaya, O. (1969), *The Mathematical Theory of Viscous Incompressible Flows*, 2nd edition edn, Gordon and Breech.

Lambert-Lacroix, S., Istas, J. & Brouste, A. (2007), 'On fractional Gaussian random fields simulations', *Journal of Statistical Software* **23**.

Langtangen, H. P., Mardal, K.-A. & Winther, R. (2002), 'Numerical methods for incompressible viscous flow', *Advances in water Resources* **25**(8-12), 1125–1146.

Lanthaler, S. & Mishra, S. (2015), 'Computation of measure-valued solutions for the incompressible Euler equations', *Mathematical Models and Methods in Applied Sciences* **25**(11), 2043–2088.

Lanthaler, S., Mishra, S. & Parés-Pulido, C. (2021), 'Statistical solutions of the incompressible Euler equations', *Mathematical Models and Methods in Applied Sciences* **31**, 223–292.

Leith, C. E. (01 Jun. 1974), 'Theoretical skill of Monte Carlo forecasts', *Monthly Weather Review* **102**(6), 409–418.

Leonardi, F. (2017*a*), 'luqness', https://gitlab.com/sam-uq/luqness.

Leonardi, F. (2017*b*), 'Sphinx', https://gitlab.com/sam-uq/sphinx.

Leonardi, F. (2018*a*), Numerical methods for ensemble based solutions to incompressible flow equations, PhD thesis, ETH Zurich.

Leonardi, F. (2018*b*), 'A projection method for the computation of admissible measure valued solutions of the incompressible Euler equations', *Discrete & Continuous Dynamical Systems - S* **11**(5), 941–961.

Leray, J. (1934), 'Sur le mouvement d'un liquide visqueux emplissant l'espace', *Acta Mathematica* **63**, 193–248.

Lévy, P. (1992), *Processus stochastiques et mouvement Brownien*, Les Grands Classiques Gauthier-Villars. [Gauthier-Villars Great Classics], Éditions Jacques Gabay, Sceaux. Followed by a note by M. Loève, Reprint of the second (1965) edition.

Lichtenstein, L. (1925), 'Über einige Existenzprobleme der Hydrodynamik homogener, unzusammendrückbarer, reibungsloser Flüssigkeiten und die Helmholtzschen Wirbelsätze', *Mathematische Zeitschrift* **23**(1), 89–154.

Lions, P.-L. (1996), *Mathematical Topics in Fluid Mechanics: Vol. 1-2*, Mathematical Topics in Fluid Mechanics, Clarendon Press.

Lye, K. O. (2020), Computation of statistical solutions of hyperbolic systems of conservation laws, PhD thesis, ETH Zurich.

Majda, A. J. & Bertozzi, A. L. (2001), *Vorticity and Incompressible Flow*, Cambridge Texts in Applied Mathematics, Cambridge University Press.

Mandelbrot, B. B. & Van Ness, J. W. (1968), 'Fractional Brownian motions, fractional noises and applications', *SIAM Review* **10**(4), 422–437.

Mishra, S., Parés-Pulido, C. & Pressel, K. G. (2021), 'Arbitrarily high-order (weighted) essentially non-oscillatory finite difference schemes for anelastic flows on staggered meshes', *Communications in Computational Physics* **29**(5), 1299–1335.

Morinishi, Y., Lund, T., Vasilyev, O. V. & Moin, P. (1998), 'Fully Conservative Higher Order Finite Difference Schemes for Incompressible Flow', *Journal of Computational Physics* **143**(1), 90–124.

Parés-Pulido, C. (2021), Statistical solutions for the incompressible Euler equations with finite volume methods, PhD thesis, ETH Zurich.

Rohner, T. (2021), Efficient implementation of spectral viscosity methods for the incompressible Euler equations (provisional title), Master thesis, ETH Zurich.

Székelyhidi, Jr, L. (2011), 'Weak solutions to the incompressible Euler equations with vortex sheet initial data', *Comptes Rendus Mathematique* **349**(19), 1063–1066.

Vecchi, I. & Wu, S. (1993), 'On L1-vorticity for 2-D incompressible flow', *Manuscripta Mathematica* **78**(1), 403–412.

Vishik, M. I., Komech, A. I. & Fursikov, A. V. (1979), 'Some mathematical problems of statistical hyromechanics', *Russian Mathematical Surveys* **34**(5), 149–234.

Wiedemann, E. (2011), 'Existence of weak solutions for the incompressible Euler equations', *Annales de l'Institut Henri Poincar C, Analyse non linaire* **28**(5), 727–730.

Yudovich, V. I. (1963), 'Non-stationary flow of an ideal incompressible liquid', *USSR Computational Mathematics and Mathematical Physics* **3**(6), 1407–1456.